Available online at www.sciencedirect.com
SCIENCE DIRECT®
Physics Reports 399 (2004) 175–225
PHYSICS REPORTS
www.elsevier.com/locate/physrep

Manipulation of large molecules by low-temperature STM: model systems for molecular electronics

Francesca Moresco*

Institut für Experimentalphysik, Freie Universität Berlin, Arnimallee 14, D-14195 Berlin, Germany

Accepted 3 August 2004
editor: J. Eichler

Abstract

The ability of the low-temperature scanning tunneling microscope to manipulate atoms and to build nanostructures with atomic precision can be extended to the manipulation of larger molecules and to selectively modify their internal degrees of freedom. Manipulation experiments on individual molecules show an exciting diversity of physical, chemical, and electronic phenomena. They permit a deeper insight into the quantum electronics of molecular systems and provide important information on the conformational and mechanical properties of single complex molecules. In this article, recent experiments on specially designed molecules will be reviewed, which investigate model systems interesting for the developing of molecular electronics. Starting from the realization of the principle of a molecular switch, going through the possibility of recording the small intramolecular changes inside a complex molecule during its movement, toward the study of the electronic contact between a single molecular wire and a metallic nanoelectrode.

PACS: 68.37.Ef; 85.65.+h; 82.37.Gk

Keywords: Scanning tunneling microscopy; Single molecule manipulation; Molecular electronics

Contents

* Tel.: +49-30-838-56465; fax: +49-30-838-51355.
E-mail address: moresco@physik.fu-berlin.de (F. Moresco).

0370-1573/$ - see front matter © 2004 Elsevier B.V. All rights reserved.
doi:10.1016/j.physrep.2004.08.001

1. Introduction

The possibility of directly interacting with a single atom has challenged scientists since the beginning of 20th century when the basic atomic constituents were discovered. At the same time, the development of quantum mechanics gave a theoretical description of the behavior of atoms and electrons. However, only with the invention of the scanning tunneling microscope (STM) in 1982 it became possible to directly "see" and "touch" an atom adsorbed on a conducting surface. The STM has radically changed the way scientists were used to interact with atoms and molecules and has allowed for the first time to build atomic structures step-by-step. The invention of Binnig and Rohrer [1–4] has not only given to the scientific community a powerful tool to image structures with atomic resolution, but it has also provided a new and general approach to the manipulation of single atoms and molecules [5–8].

However, the fascinating possibility of building complex functional structures by manipulating atom by atom can be taken even a step further. The ability of low-temperature STM (LT-STM) to manipulate atoms and small molecules can be extended to the manipulation of larger molecules and to selectively modify their internal degrees of freedom. Experiments on individual molecules show an exciting diversity of physical, chemical, and electronic phenomena. They permit a deeper insight into the quantum electronics of molecular systems and provide important information on the conformational and mechanical properties of single complex molecules [9–12].

Such experimental abilities ideally match the present challenges in nanoelectronics, which is currently focusing on the possibilities offered by single molecules [13]. Lithographic techniques used in today's production of miniaturized silicon-based transistors will probably soon reach their limit and the size of electronic circuits will need to have the scale of atoms, a goal that requires conceptually new device structures. A fundamentally new approach is needed for the rapid handling of vast amounts of information on

the nanometer scale. Such a demand for increasingly sophisticated technologies is encouraging scientists to think more intensely on the molecular scale in the quest for more efficient ways of writing, storing, processing, reading, and transferring information [14,15].

The idea that a single molecule can be embedded between electrodes and perform the basic functions of digital electronics (rectification, amplification, and storage) was first put forward in the mid-1970s. Aviram and Ratner proposed in 1974 a rectifier consisting of a single molecule [16]. They suggested that a molecule with a donor–spacer–acceptor structure would behave as a diode when placed between two electrodes, demonstrating the first hybrid molecular electronic device comprising molecules embedded between several electrodes [14].

In the late 1970s and early 1980s biochemists began using natural biological processes to build and manipulate proteins and other biologic molecules [17,18], opening the way to the manipulation of single DNA molecules and to the direct measurement of their mechanical properties [19–21].

In the 1980s physicists were experimenting with many new quantum structures. They were capturing single electrons in potential wells, called "quantum dots" [22–24]. Quantum effects were also at the basis of scanning tunneling microscopy and atomic force microscopy [1–4,25]. By means of STM it became possible to perform controlled two-terminal measurements on molecules, opening new experimental approaches for demonstrating and probing electron transport through individual molecules [26,27]. Some examples are in this respect the electrical single-atom switch realized using a Xe atom [28] at cryogenic temperature and the first experimental determination of the electrical contact point of a single C_{60} molecule [11]. STM measurements on C_{60} have shown linear current-voltage characteristics at low applied voltage. However, by pressing a C_{60} molecule applying a small force with a metallic STM tip, produces a shift of the molecular orbital levels, which results in a modulated tunneling current through the single C_{60} molecule. The phenomenon can be used to design an electromechanical amplifier [29].

The conductance through single molecules, whose configuration mimics the planar wiring configuration characteristic of semiconductor devices, has been investigated by means of a variety of other techniques, and experiments based on Coulomb blockade [30–32], nanopore [33], break junctions [34–36], electrodeposition [37], and nanolithography [38,39] have been recently reported. An important experiment in this respect is the measurement of the conductance of single-wall carbon nanotubes. It represented the first observation of a molecular-scale object electrically interconnected in a full planar configuration [40–44]. Single wall carbon nanotubes with appropriate helicity are found to transport electrons ballistically [40]. Consequently, the conductance of the metal–nanotube–metal junction is determined and limited by the metal–nanotube contacts. It is generally difficult to decrease contact resistances in this system below 100 Ω [45]. Break junctions involve the fracture of a micro-fabricated electrode in its center by mechanical deformation while measuring the resistance of the metallic wire junction [46]. Its application to single molecules is not straightforward because the conformation and the exact number of interconnected molecules remain difficult to determine [36]. Nevertheless, some recent experiments have shown the possibility of investigating the transport through molecules by means of the break junction method, when the molecules are strongly coupled to gold electrodes by means of thiol groups [47].

In the last years the convergence of development in physics, chemistry, biochemistry, electrical engineering and computer science began to form a route toward a practical, useful nanotechnology. Methods have become available for positioning single atoms [5,6,28,48], billions of copies are routinely made of identical molecules and great strides have been made in the self-assembly of more complex structures from molecular building blocks [49–53] and in patterning nanostructures [54,55]. In the last decades enormous progress has been done in growing ultrathin films of organic molecules and in understanding

their modes of growth [56]. Self-assembly presently appears to be a practical strategy for fabricating ensembles of molecular nanostructures in a parallel geometry. Moreover, self-assembled organic thin films have a number of practical applications, ranging from sensors [57] to heterogeneous catalysis [58] to biomaterial interfaces in medical implants [59]. Self-assembled supramolecular nanostructures can be built at surfaces by means of hydrogen bonding. By using STM, the adsorption of PVBA on a silver surface has been recently characterized showing that a one-dimensional supramolecular nanograting can be fabricated on Ag(1 1 1) by a cooperative self-assembly process [60].

This short historical review shows how the common image of microelectronics and computation has radically changed in the last decades. The dimension of synthetic molecular systems is now comparable with the levels of miniaturization in microelectronics and with the length scale of biological systems. This suggests that a "bottom-up" approach to nanofabrication may one day compete with conventional "top-down" approaches. It is however important to note that the application of conventional electronic concepts to molecules is not straightforward: Molecules are quantum mechanical objects, operating on a dimensional scale where quantum mechanics dominates. A standard circuit analysis resulting from the application of Ohm's and Kirchhoff's laws is not applicable to molecules, even if the design of molecular logic continues to be based on those laws [61]. Contrary to conventional electric circuits, in fact, where adding one branch does not change the electronic properties of the others, any new molecular wire or branch added to a molecule effectively creates a new molecule with a different electronic structure. New approaches have then to be found, able to achieve functional molecular devices by exploiting their quantum mechanical properties.

The idea of fabricating nanoscale devices combining the new possibility of molecular synthesis with the capability of controlled manipulation of single atoms is now challenging the scientific community. Many interesting and fascinating prospects are in front of us. For example, the possibility of directly computing inside a single molecule. The idea is to build "monomolecular" electronics, in which a single molecule will integrate the elementary functions and interconnections required for computation. In this frame LT-STM is coming up as a fundamental technique to investigate mechanical and electronic properties of single molecules and to realize prototypes of molecular machines and molecular electronic devices.

An open problem in the development of molecular electronics remains the difficulty in mastering the electronic contact to a single molecule. This subject will play a key role in the fabrication and the performance of molecular devices. In a molecular electronic device, in fact, a crucial problem is the observation and control of the contact of the active molecular unit with its electrodes [34,62]. The quality of such a contact relies on the precise electronic interaction between the end groups of this active part and the surface of each electrode [63–65]. With its sub-nanometer resolution, LT-STM allows to investigate in detail the contact between a single molecule and a metallic electrode. This opens the way to the optimization of the molecular termination, with the aim of reaching low conductance contacts.

In this article, a review on recent LT-STM manipulation experiments of specially designed molecules is presented. After an introduction of the scanning tunneling microscope and its application to the manipulation of single atoms and small molecules, the extension of the lateral manipulation techniques to large molecules will be presented. This results in a vast and interesting range of perspectives: starting from the realization of the principle of a molecular switch working under the action of a STM tip, going through the possibility of recording the small intramolecular changes inside a complex molecule during its movement, toward the idea of controlling the mechanics of a molecule and the realization of molecular

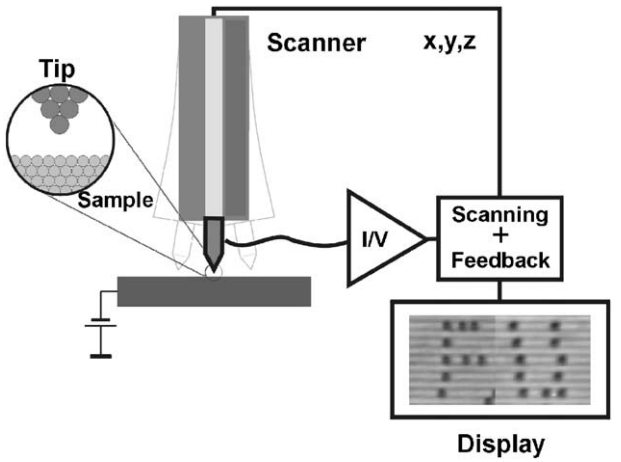

Fig. 1. Working principle of a scanning tunneling microscope.

nano-robots. Finally, I will show how the electronic contacting and de-contacting of a molecular wire to a metallic step edges and atomic metallic wires can be controlled by manipulation.

2. Experimental

In all the experiments described in this article, a home-built, versatile STM is used, capable of operation between 7 and 300 K and working in ultra high vacuum (UHV) conditions. A detailed description of the first home-built instrument can be found in Ref. [66], while the instrument used in the present work is described in Ref. [67].

The fundamental part of an STM is a sharp metallic tip ending ideally in a single atom [68]. The tip is brought very close to the sample surface and can be scanned laterally by piezoelectric tubes. The working mode of the STM is shown in Fig. 1. When the tip is positioned in an atomic distance (about 5–10 Å) over the surface, the application of a bias voltage of some mV between tip and sample leads to the flow of a tunneling current of several nA. The ability of the STM to image surface topography with atomic resolution is based on the fact that this tunneling current is a very sensitive, exponential function of the tip–sample distance. Typically, the current changes by an order of magnitude for a change in tip–sample distance of 1 Å. As a result, the current flows predominantly through the few atoms of the tip, which are closest to the sample surface, yielding high lateral and vertical resolution.

In the most common working mode the current is kept constant by a feedback system. Because the tunneling current is extremely sensitive to the tip–sample distance, the tip follows the corrugation of the surface when it is moved parallel to it. The vertical position of the tip as a function of the horizontal position gives rise to a locally resolved image of the atomic distribution on the surface. In reality it shows the local electronic density at the surface, which however in the case of a metallic sample reflects the geometrical order of the atoms [68,69].

The UHV chamber which hosts the STM works at a base pressure of 10^{-10} mbar is shown in the photo of Fig. 2. It is divided in two parts by an UHV valve: the left part is used for sample preparation, while the

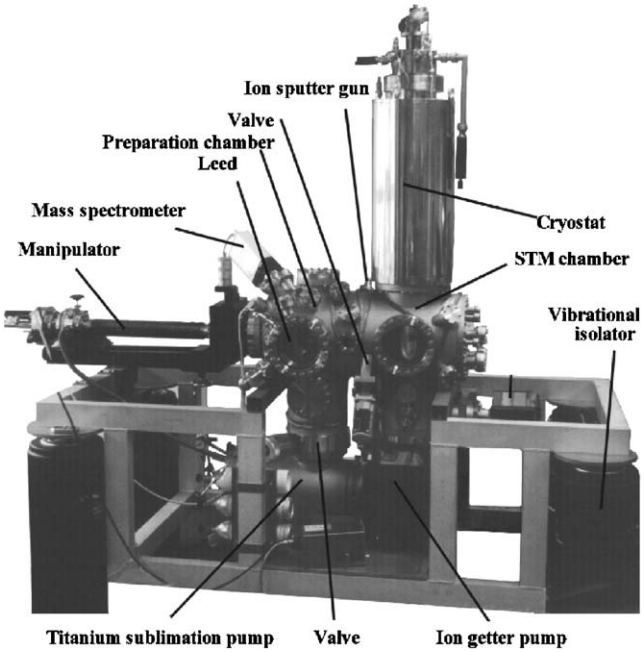

Fig. 2. UHV chamber. The left part (preparation chamber) and the right one (STM-chamber) are separated by a valve. A liquid helium cryostat allows cooling the crystal down to 7 K. The system is placed on pneumatically isolating feet.

right part contains the microscope itself. The preparation chamber is equipped with ion sputtering gun, LEED, mass spectrometer, and several evaporators. Inside the chamber it is possible to store two sample holders. A magnetic transfer rod can be mounted to transfer a sample in and out of the UHV chamber without breaking the vacuum. A manipulator is used to transfer the sample into the STM chamber. It can be moved in all three spatial directions and rotated around its axis. The top end of the manipulator can be cooled down to about 15 K.

The cryostat system allows the STM to be cooled down to about 7 K. It consists of an inner part, which can be filled by with 4.3 l of liquid helium with a consumption time rate lower than 0.1 l/h and of an outer tank, filled with 13.3 l of liquid nitrogen. Both tanks are surrounded by thermal radiation shields of aluminum. Such radiation shields surround the STM as well and operate as a cryopump, maintaining in the STM a pressure well below 10^{-10} mbar and allowing the sample to remain clean for a long period of time.

The STM has high mechanical stability and good drift compensation. It is composed, as shown in Fig. 3, of three piezoelectric tubes holding, through three sapphire balls, a copper plate. A further piezoelectric tube placed in the center of the base supports the tip. If the three piezos move in the same direction, the approach ring will follow this movement, giving rise to a vertical movement of the tip used for coarse approach. To perform a scan parallel to the surface the lateral piezoelectric tubes are used, while the fine regulation of the tip–surface distance is done by the central piezo. The amplitude of movement of the piezoelectric tubes is about 10 Å/V. The voltage applied to the piezos can vary between 1 mV and 100 V. This corresponds to a maximal resolution of about 0.01 Å for a scan range of 1 μm.

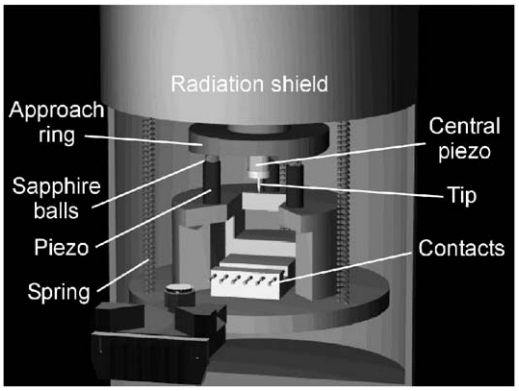

Fig. 3. STM inside the radiation shields. The piezoelectric tubes and the contact pads are indicated.

To achieve a good mechanical isolation against vibrations, the microscope hangs on helical springs. These are connected to the lower part of the liquid helium cryostat. Isolation against external vibrations is obtained placing the whole system on pneumatic isolators (visible in the photo of Fig. 2) with resonant frequency below 2 Hz. During STM measurements all mechanical pumps are switched off.

The sample is mounted on a copper sample holder, which can be fixed on the manipulator and placed inside the STM. In its back part, the sample holder has a ceramic plate covered by conducting pads, which are used to achieve the electrical contact to the manipulator for heating the sample and measuring its temperature by a Ni/Cr–Ni thermocouple. In addition, they permit to apply the bias voltage when the sample is inside the STM. The sample is mounted on an oven, for heating the crystal up to about 1000 K.

As substrates for our manipulation experiments we used the low-Miller-index copper surfaces Cu(1 1 1), Cu(1 1 0) and Cu(1 0 0), and the regularly stepped Cu(2 1 1), which consists of (1 1 1)-nano-facets separated by (1 0 0)-steps of monoatomic height. The crystals are prepared in UHV by several cycles of sputtering with Ne-ions and annealing at about 700 K.

The tip is prepared from tungsten wire (thickness 0.25 mm) by electrochemical etching before it is put into the UHV chamber. The tip is then sharpened and cleaned by controlled crashing into the metallic surface. Therefore the tip can be considered, in the following, covered by copper atoms.

The molecules investigated in this article are evaporated onto the surfaces in UHV conditions from a metallic crucible resistively heated to temperatures between 550 and 600 K. The temperature of the crucible is measured by a Ni/Cr–Ni thermocouple.

The evaporation system is developed for the deposition of the large molecules described in the following and is mounted to the preparation chamber, separated from it by a UHV valve. It is differentially pumped by a turbo pump. This geometry allows us to introduce molecules in the crucible and to degas them up to 550 K without degradation of the chamber pressure. The degassing procedure is carefully controlled by measuring the pressure in the separated evaporation chamber and the amount of evaporated material is controlled by a quartz microbalance. The described procedure permits to deposit sub-monolayer amounts of molecules on clean metallic surfaces maintained either at room temperature or cooled down to 80 K. The absolute coverage is directly determined by STM.

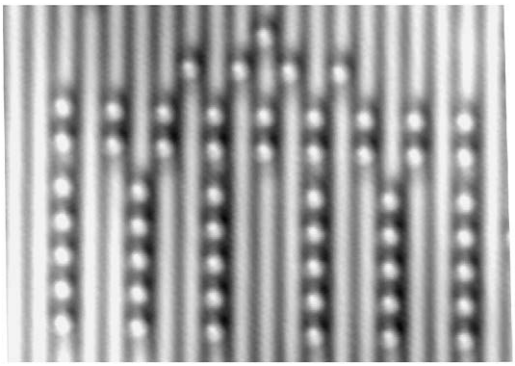

Fig. 4. An example of lateral manipulation: STM image of the Brandenburg Gate in Berlin realized by CO molecules on Cu(2 1 1). Substrate temperature: 15 K. Size of the image: 125×95 Å^2. From Gerhard Meyer, with permission.

3. Manipulation of single atoms and small molecules

Soon after the first STM experiments it was realized that, upon scanning, the tip often modifies the substrate because of its close proximity to the surface atoms. This obvious disadvantage for imaging can be however turned into a positive prospect by realizing that the modifications can be made in a controlled way [5,6]. At cryogenic temperature, the tip of an STM can be used to build atomically precise nanostructures and allows investigating the motion of single atoms and molecules. In this section a short review on the manipulation of single atoms and small molecules will be presented.

The basic techniques, which allows to transport atoms and small molecules by means of the STM-tip for the formation of nanostructures involve either moving a single particle to the wanted position without losing the contact to the surface (lateral manipulation) or picking it up with the tip and depositing it at the desired location (vertical manipulation).

The manipulation process can be controlled by varying three main parameters in the STM: the electric field, the tunneling current, and the forces between tip and surface [6]. For the lateral manipulation at atomic scale, the interaction forces between tip and atom, i.e. van der Waals or chemical forces, are sufficient to move an atom and no electric field or current are applied. On the other hand, field and current effects play a major role in vertical manipulation. Both types of manipulation were used for the first time by the group of Don Eigler at IBM-Almaden [5] and then in Berlin [7,70] to build nanostructures from single atoms and molecules. Methods to manipulate strongly bounded atoms (like Br) at room temperature have been recently developed by Pethica et al. [71].

An example of an artificial structure created by lateral manipulation is shown in Fig. 4. The Brandenburg Gate of Berlin is reproduced at the atomic scale. The structure was built by manipulating CO molecules laterally on Cu(2 1 1). Because of the high thermally induced mobility of the molecules, it was necessary to work at low temperature. The experiment reported in Fig. 4 was performed at 15 K. At this temperature the diffusion of many adsorbates on metallic surfaces is prohibited and it is possible to work with a rather large number of particles. The diffusion of CO molecules has been studied in detail by STM on Cu(1 1 0) as a function of temperature and the activation energy for the thermal motion directly determined [72].

In Fig. 5 different stages of the construction of another artificial nanostructure of CO molecules deposited on Cu(2 1 1) are shown. The area was initially prepared by removing the CO molecules by lateral

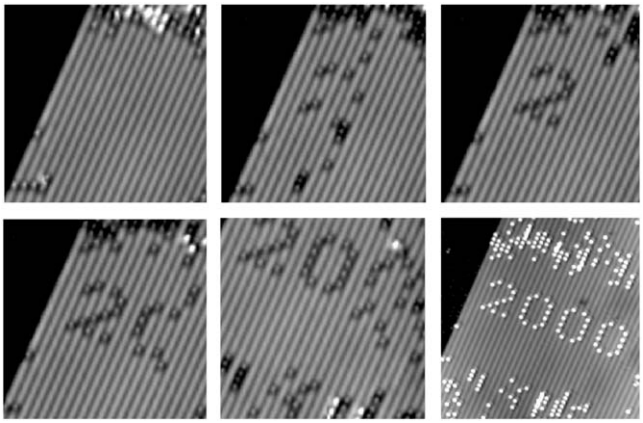

Fig. 5. Sequence of STM images showing the gradual construction of the number “2000” with 47 CO molecules on a Cu(2 1 1) substrate. Note that an area free of CO molecules had to be prepared by manipulation in the beginning. The changed contrast in the last image is caused by the transfer of a CO molecule to the STM tip. From Jascha Repp, with permission.

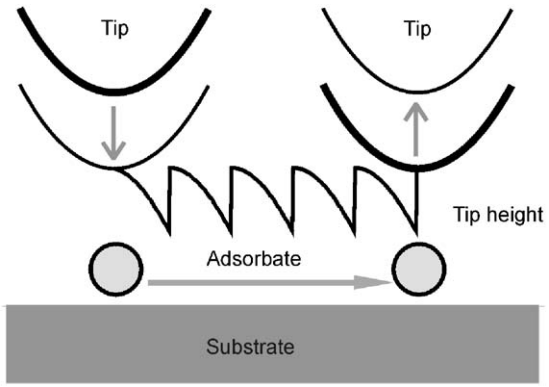

Fig. 6. Sketch of the lateral manipulation process in constant current mode. The tip height curve carries information about the movement of the adsorbate on the surface.

manipulation. The structure was then built molecule by molecule. It is interesting to note that in the last image of Fig. 5 the molecules appear like protrusions while in the previous images they look like depressions. This is due to the fact that between the two images the tip picked up a CO molecule by vertical manipulation, giving rise to the observed change in the appearance of the molecules. As recently reported [73], the transfer of a CO molecule onto the STM tip can be performed in a controlled way and leads to an enhanced chemical contrast. The presence of a CO molecule on the tip apex allows one to distinguish an adsorbed CO molecule from other adsorbates, like for example oxygen atoms, which look similar when imaged with a bare metal tip.

Fig. 6 shows the typical process for the lateral manipulation of small molecules and single atoms. To perform lateral manipulation, the tip is first positioned above the adsorbate and its distance to the surface is reduced to 2–4 Å by increasing the set-point current by approximately two orders of magnitude at a bias

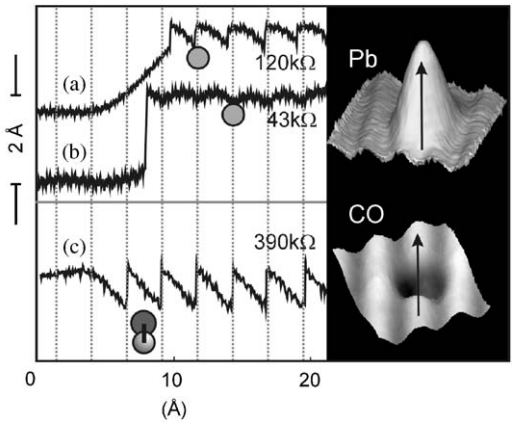

Fig. 7. Tip height curves recorded during the manipulation of a Pb atom ((a) and (b)) and a CO molecule (c) along the intrinsic step edges of Cu(2 1 1). The tip is moved from left to right and the respective tunneling resistances are indicated. The vertical dotted lines correspond to fcc sites. It is possible to distinguish between three different modes: (a) pulling, (b) sliding, and (c) pushing. Reprinted with permission from Ref. [48]. Copyright 1997 by the American Physical Society.

voltage of about 10–100 mV. The tunneling resistance is thus reduced from about 10 MΩ in the imaging mode to a few 100 KΩ in the manipulation mode. The process is then performed in constant current mode and the particle is dragged by the lateral movement of the tip to the chosen final position. Reducing the tunneling current, the tip finally retracts to a height characteristic for the normal imaging mode. The usual manipulation velocities are 10–100 Å/s.

As one can see in Fig. 6, corresponding to the jumps of the adsorbate from an adsorption position to the next, the tip height oscillates periodically during the manipulation in order to keep the tunneling current constant during the process. By recording the curve of the tip height during the manipulation it is possible to recognize three different types of lateral manipulation: pushing, pulling, and sliding [48]. The different behavior depends on the tip–particle force, which determines the position of the adsorbate under the tip during the manipulation. The three different manipulation types can be recognized in the examples reported in Fig. 7.

During a pulling process (Fig. 7(a)) the adsorbate is situated behind the tip apex with respect to the manipulation direction. The atoms are manipulated via an attractive tip–adatom interaction and follow the tip discontinuously by hopping from one site to the next. This is the case for Pb (and also for Cu) atoms on Cu(2 1 1).

Upon a further reduction of the tunneling resistance, Pb atoms can also be manipulated attractively in a continuous way (sliding mode, Fig. 7(b)). During a sliding process, the adsorbate remains bound under the tip apex without escaping from the defined trajectory. The tip–particle interaction is so strong in this case that tip and particle form a composed system, which scans the corrugation of the substrate.

Finally, single CO molecules, as well as many other small molecules, can be manipulated reliably via repulsive interaction (pushing mode Fig. 7(c)). During a pushing process the adsorbate is in front of the tip and it is pushed by the advancement of the tip apex due to a repulsive interaction. It is important to note that in the attractive manipulation modes (pulling and sliding, Fig. 7(a) and (b)) the particle first hops toward the tip and then follows it, while in the repulsive mode (pushing, Fig. 7(c)) the particle performs hops away from the tip.

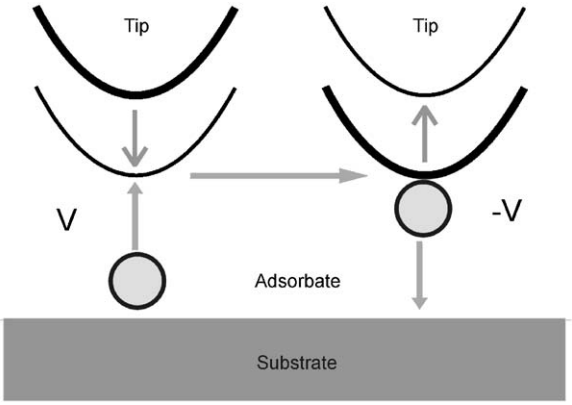

Fig. 8. Sketch of the vertical manipulation procedure. To transfer an adsorbate to the tip and deposit it in the final position a voltage pulse is applied when the tip–surface distance is decreased.

By recording the manipulation signal of single copper adatoms on Cu(1 1 1) [74] it has been possible to extract very fine details during the manipulation process. The adsorbate shows various movement patterns visiting different surface sites upon the application of different tip forces. This result demonstrates that the analysis of the manipulation signal is a powerful tool to investigate the mechanics of a molecule on a surface when guided by the tip and its interaction with a metallic surface.

Vertical manipulation was first performed in the group of Eigler [28]. They demonstrated that a Xe atom could be reversibly transferred between the tip and the surface by the application of a voltage pulse. The principle of the vertical manipulation of an adsorbate is shown in Fig. 8. To transfer the atom to the tip a voltage is applied and contemporarily the tip–surface distance is decreased. The tip is then retracted and moved to a chosen position, where lowering the tip and applying a voltage pulse of opposite polarity release the adsorbate.

Vertical manipulation experiments have been recently performed also on semiconductor surfaces, showing that Ge atoms can be extracted from a Ge(1 1 1) surface [75] and that the formed vacancy exhibits a selective reactivity toward molecular oxygen [76].

Another example of vertical manipulation is given by CO molecules on copper surfaces [73]. The CO molecule stands upright on the copper surface with the carbon atom binding to the substrate and it has to turn around when being transferred to the tip. A reliable procedure to transfer the CO to the tip is to apply a voltage of a few volts and simultaneously to decrease the tip–surface distance. A detailed analysis of the vertical transfer mechanism of CO molecules on Cu(1 1 1) shows that a minimum tunneling bias of 2.4 V is required to start the process [77].

The described ability of transferring a CO molecule to the tip by vertical manipulation not only increases the chemical contrast of the tip, but allows to control its shape and to significantly enhance the tunneling current through an adsorbed molecule and therefore to change the sensitivity for inelastic tunneling, making possible to detect the vibrational excitations of isolated CO molecules [78].

Whereas spectroscopy of electronic states employing the STM was used already in 1985 [79], vibrational spectroscopy was performed for the first time only in 1998, when the group of Ho [80] showed that the C–H stretch mode could be observed on single C_2H_2 molecules adsorbed on a Cu(1 1 1) surface. Later a number of systems have been characterized by vibrational spectroscopy [81] including larger

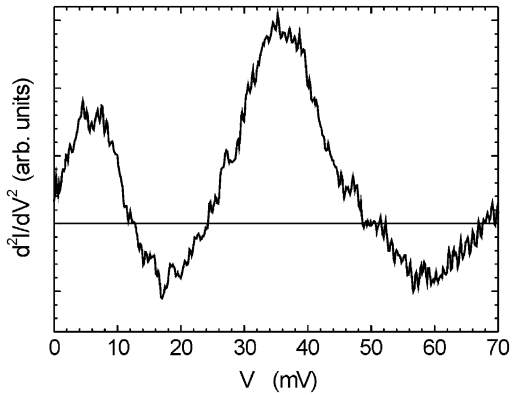

Fig. 9. Vibrational spectroscopy with a CO-functionalized tip. The d^2I/dV^2 spectrum of a single CO molecule on Cu(1 1 1) exhibits the frustrated translational and rotational modes.

molecules such as ethioporphyrin-I on Cu(0 0 1) [82], water on Ag(1 1 1) and Cu(1 1 1) [83], as well as single atoms like H and D on Cu(0 0 1) [84] or *trans*-2-butene molecules [85].

With a CO terminated tip we have observed the frustrated translational and vibrational excitations of isolated CO molecules adsorbed on Cu(2 1 1) [78]. In Fig. 9 the vibrational spectrum measured in our experiment is shown, obtained after having transferred a single CO molecule on the tip by vertical manipulation. The frustrated rotational and vibrational modes of CO on Cu(2 1 1) are observed at energies of 5.8 and 35.9 meV, respectively.

The vibrational modes of CO deposited on Cu(1 0 0) have been recently observed also using a metallic tip [86]. The frustrated rotational and the frustrated translational mode have been resolved, while the CO-metal vibration could not be detected. In our case, the presence of a CO on the tip strongly influences the frustrated translational mode of the CO molecule, which shifts toward higher energy, while it does not affect the frustrated rotational mode. Moreover, the selection rules of the vibrational modes are apparently not affected by the presence of the CO on the tip.

More generally, the ability of picking up a single atom or molecule on the tip apex opens the way to control the shape of the tip, to significantly enhance the tunneling current through the molecule and therefore to change the sensitivity for inelastic tunneling. Moreover, by studying the vibrational modes of a molecule with different kinds of tips, it may be possible to modify the selection rules for the observation of the excitation modes.

The combined application of the different manipulation techniques opens the possibility of inducing the steps of a complex chemical reaction with the STM tip [87]. Specifically, the synthesis of biphenyl from iodobenzene on copper (Ullmann reaction) has been induced using the STM tip at 20 K and a Cu(1 1 1) substrate. The reaction essentially consists of three steps: dissociation of iodobenzene (C_6H_5I) to phenyl (C_6H_5) and iodine, diffusion of phenyl to find another phenyl molecule as a reaction partner, and their chemical association to form biphenyl ($C_{12}H_{10}$). In the reported STM experiment, shown in Fig. 10, the iodine atoms originating from two C_6H_5I molecules adsorbed at a Cu(1 1 1) step were separated from the parent molecules by injecting tunneling electrons at 1.5 eV. Iodine and phenyl were further separated with the tip. Then, the iodine atom located between the two phenyls has been removed to the lower terrace by using lateral manipulation. The left phenyl is then repositioned close to the right phenyl by pulling

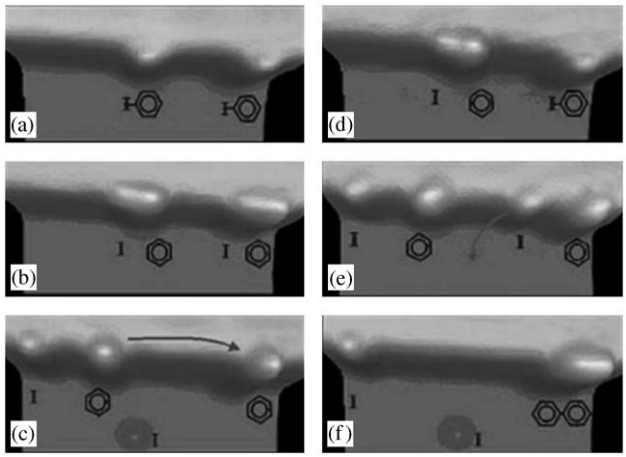

Fig. 10. STM images showing the steps of the tip-induced Ullmann reaction. (a) Two iodobenzene molecules are adsorbed at a Cu(1 1 1) step edge. (b), (c) Iodine is separated from both molecules using a voltage pulse and (d) further manipulated. (e) The iodine atom located between the two phenyls is removed. (f) The two phenyl molecule are brought together by manipulation and then associated by a voltage pulse. Reprinted with permission from Ref. [87]. Copyright 2000 by the American Physical Society.

with the tip. The injection of tunneling electrons with an energy of 500 meV achieved the formation of a chemical bond of the two phenyls. The formation of biphenyl is verified by pulling the synthesized molecule at its front end with the tip. The experiment constitutes an important step toward the assembly of individual molecules from simple building blocks in situ at the atomic scale.

Very recently, some interesting experiments have shown how lateral manipulation of single atoms or small molecules can be applied to the investigation of more complex problems. Nilius et al. [88] have studied the development of the one-dimensional band structure in gold chains, artificially formed by lateral manipulation on a NiAl(1 1 0) surface. Heinrich et al. [89] have shown how CO molecules can be arranged by lateral manipulation to form kind of "molecular cascades", where the motion of one molecule causes the consequent motion of the another, and so on. The experiment exploits the motion of individual molecules on surfaces in nanometer-scale structures and allows to implement very small models of logic circuits.

4. TBPP and Lander: molecules designed for manipulation

Scanning tunneling microscopy has been in the last years intensively applied to the imaging of individual molecules [90] and the possibility of experimentally identify the molecular conformation and adsorption geometry of a single molecule on a surface [91] has been combined with manipulation techniques and used to investigate mechanical and electronic properties of individual molecules.

The manipulation of single molecules and its application to the development of electronic and mechanical devices requires first of all a range of suitable molecules. For each purpose, i.e. to build molecular electronic devices or mechanical nano-machines, special molecules need to be designed and synthesized. In the last years there have been a renewed interest in the construction of well-defined macromolecules.

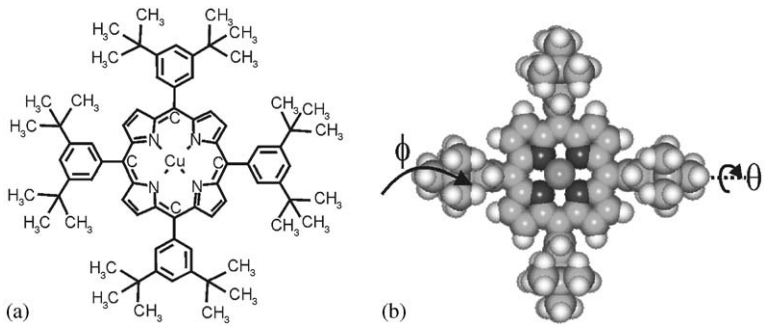

Fig. 11. (a) Chemical structure of the TBPP molecule. For clarity of the chemical constitution the legs are shown parallel to the porphyrin ring. (b) Sphere model of the molecule as it appears in the gas phase. The legs are now rotated at $\theta = 90°$. The rotational degrees of freedom of the single legs, used to optimize the conformation geometry, are defined. θ is the rotation of a leg around the σ-bond and ϕ indicates the bending of this σ-bond. The molecule has in the gas phase a diameter of about 25 Å and is about 9 Å high.

As a result, modern synthetic chemistry has been intensively applied to the construction of this class of composts [92].

The molecules described in the following have been specially designed to be investigated by STM and to study the effects of LT-STM manipulation on the internal conformation of the molecule. They can be considered model systems for molecular switches and conducting wires kept isolated from metallic surfaces.

The first molecule we want to present is called *Cu-tetra-3,5 di-ter-butyl-phenyl porphyrin* (and it will be called in the following TBPP). It is a specially designed porphyrin based molecule [93] with four phenyl-based lateral groups. Its chemical structure is shown in Fig. 11(a). The four lateral groups form legs, which electronically decouple the porphyrin central ring from the metallic surface. As shown in the model of Fig. 11(b), in the gas phase the legs are oriented perpendicular to the central ring, but are able to rotate around the s-bond connecting each of them to the porphyrin, adapting themselves to the substrate corrugation.

As one can see in the STM images reported in Fig. 12, the molecule shows four bright lobes corresponding to the legs, while the central ring is not visible because the π-orbitals of the porphyrin are electronically decoupled from the metal surface and the tunneling current flows mainly through the legs. The adsorption geometry of TBPP on Cu(1 1 1), Cu(1 0 0), and Cu(2 1 1) has been investigated in detail by LT-STM and the angular rotations of the lateral groups in the different cases has been determined [94]. Previous experiments at room temperature have already allow to observe different conformations of the molecule on different substrates [95].

On Cu(1 1 1) (Fig. 12(a)) the molecule shows eight lobes reflecting the four legs lying flat on the surface. The legs are oriented in parallel to the porphyrin plane and the two butyl end groups of each leg interact with the surface, giving rise to a corresponding double maximum. The molecule shows a symmetry axis corresponding to the closed packed directions of the substrate and three different equivalent orientations of the molecule are possible, rotated of 60° with respect to each other. The presence of a symmetry axis in correspondence with the closed packed direction of the substrate indicates that the four-fold symmetry expected from the molecular structure of the TBPP has been broken to permit the molecule to adapt itself to the substrate.

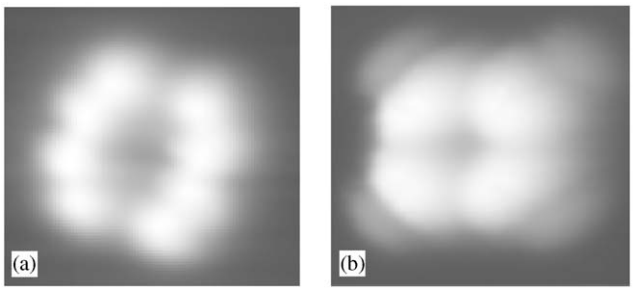

Fig. 12. STM images of a TBPP molecule deposited (a) on Cu(1 1 1) and (b) on Cu(1 0 0). In both cases the molecules show a diameter of about 25 Å. In (a) the molecule lies flat on the surface and shows two bumps per leg, each having an apparent height of 2 Å. In (b) on the contrary the legs are nearly perpendicular to the surface, have a single maximum, and an apparent height of 4 Å.

In contrast, on Cu(1 0 0) the TBPP molecules are adsorbed in only one orientation, which follows the high symmetry [1 −1 1] direction of the substrate. The molecule shows only four bright lobes and the legs are oriented nearly perpendicular to the porphyrin ring, showing a conformation very similar to the one in the gas phase (Fig. 12(b)). There are essentially two parameters per leg controlling the molecule conformation on Cu(1 0 0): the rotation θ and the bending ϕ described in Fig. 11(b). In particular, we found that on Cu(1 0 0) each leg is rotated with respect to the central porphyrin ring by $\theta = 80°$ and $\phi = 30°$. The explanation for these two rotations is that, upon adsorption, the central porphyrin is attracted toward the surface by a van der Waals interaction. This attraction forces the porphyrin to approach the surface and puts a constrain on the legs, which is shared between θ and ϕ. The bending ϕ results slightly larger than the rotation θ because of the steric crowding between the hydrogen of a given leg phenyl group and the central porphyrin.

On Cu(2 1 1), the molecules show in most cases eight bright lobes corresponding to four legs oriented nearly flat on the surface, with two different preferential orientations on the surface. In a few cases and for both adsorption configurations, a leg appears as a brighter single lobe. In these cases a leg is rotated around the σ-bond out of the plane of the central porphyrin ring. The different orientations of the lateral groups on Cu(2 1 1) will be described in details in Section 7.

TBPP was the first example of a single intact molecule to be precisely positioned by means of manipulation with the STM tip at room temperature. The experiment was performed by Jung et al. [10] at IBM-Zurich. Some STM images corresponding to different stages of the manipulation are reported in Fig. 13. The controlled positioning of TBPP at room temperature was possible because of the special architecture of the molecule, where the lateral groups permit a sufficiently strong interaction of the molecule with the surface preventing thermally activated diffusion and, on the other hand, decouple the central part of the molecule from the substrate allowing its controlled translation. The experiment demonstrates that the special design of the molecule, where functional groups are attached to a rigid planar molecule, allows maintaining stable bonding, while being sufficiently labile to facilitate tip-induced translation without braking internal molecular bonds.

The second molecule we have investigated is called molecular Lander ($C_{90}H_{98}$) [96] and consists of a long rigid polyaromatic main board (a molecular wire), maintained above the surface by four TBP (di-ter-butyl-phenyl) spacer groups, which are exactly the same lateral groups already described in the

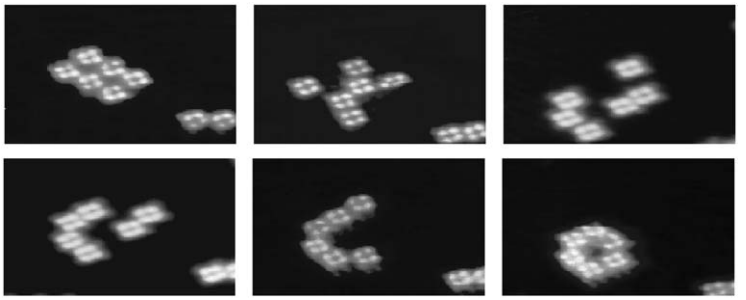

Fig. 13. Different stages of the manipulation of TBPP by STM at room temperature. Each molecule is individually repositioned to form a nearly hexagonal ring. Reprinted with permission from Ref. [10]. Copyright 1996 AAAS.

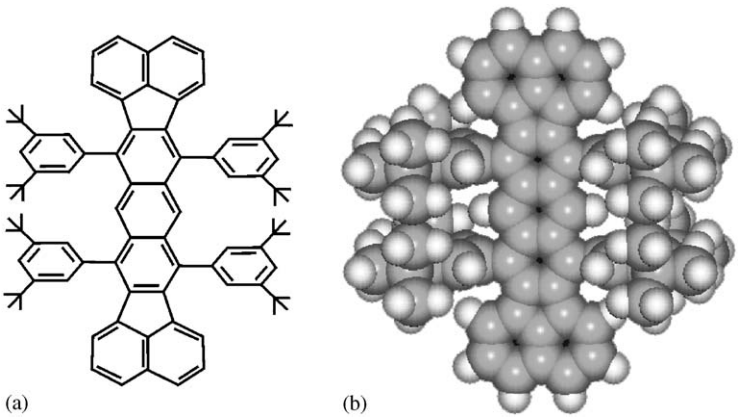

Fig. 14. (a) Chemical structure of a Lander molecule. (b) Space-filling representation of the conformation of a Lander: As shown in the model, in the gas phase the legs are maintained perpendicular to the central board by steric repulsion.

case of TBPP. The design of the Lander guarantees the separation of the board from the metal surface to preserve its electronic integrity and to allow the manipulation with the STM tip. Moreover, the main board has a rigid aromatic platform projected beyond the last spacer, which is useful to study the electrical contact with a terrace or a nanostructure on a metal surface. The chemical structure of the molecule and a sphere model are shown in Fig. 14. The similarity between these molecular ladders and landing craft such as the Mars Lander had led to the name “molecular Landers” [96].

The Lander molecule was specially designed to study the electrical properties of the central molecular wire by STM [63]. As in the case of TBPP, the lateral groups of the Lander are oriented perpendicular to the central board in the gas phase, but adapt themselves to the surface structure when the molecule is deposited on a surfaces, showing different orientations [97–100]. On all the investigated copper surfaces, the molecule appears as four bright lobes in STM images, similarly to the case of TBPP. The tunneling occurs in fact primarily via the lateral TBP groups, while the central molecular wire contributes very little to the tunneling current. Due to the symmetry of the σ bond between the TBP groups and the central wire, the spacer legs can rotate around the bond axis. When the molecule is adsorbed on a surface and due to steric hindrance, the legs positioned on the same side of the central molecular wire always rotate in the

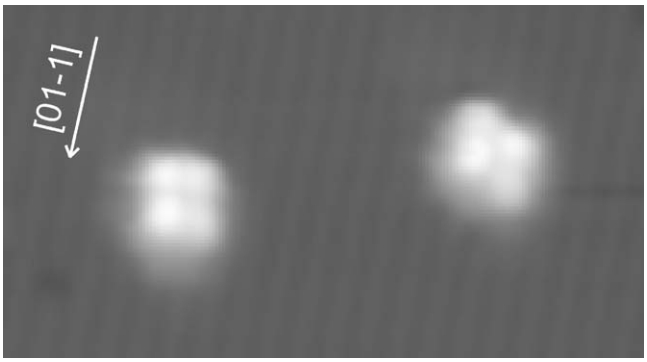

Fig. 15. Experimental STM images of two Lander molecules deposited on Cu(2 1 1). The direction of the intrinsic steps, slightly visible in the image, is indicated. The size of the image is about 110 × 60 Å.

same direction, resulting in two qualitatively different conformations. In one case, the two legs on both sides of the central wire rotate in the same direction. This conformation is called parallel-leg conformation and it leads to a square shape of the molecule in STM images. In the second case, the legs on both sides rotate in opposite directions. This is called the crossed-leg conformation. It leads to a rhombic shape in the STM images.

The STM images shown in Fig. 15 have been recorded for Landers adsorbed on Cu(2 1 1). The two described configurations are visible. In one case the molecule shows a square form and has the legs oriented parallel to each other (parallel-leg conformation, left molecule in Fig. 15). In the second case it has a rhomboidal form (crossed-leg conformation, right molecule in Fig. 15). Calculations demonstrate that in both cases the legs are rotated and that the distance between the central board and the metallic surface is only 3.7 Å, compared to the 7 Å expected for the conformation observed in the gas phase. The orientation of the board is determined by the comparison between the calculated and the experimental images [97]. The board is parallel to the direction of the shorter distance between two legs, i.e. the molecule appears wider than longer. The example in Fig. 15 shows a molecule (the left one) with the board oriented perpendicularly to the Cu(2 1 1) intrinsic steps and the other (the right one) having the board in the direction of the rows [100].

It is important to note that TBPP molecules deposited at room temperature on copper surfaces are found randomly distributed on the terraces, while Landers adsorbed at the same temperature are found exclusively located at step edges. This result indicates a lower diffusion barrier for the Lander molecule compared to the TBPP and is probably due to the better adaptability of the TBPP to the surface corrugation and to an attractive interaction between the porphyrin ring and the Cu surface. As it will be shown in the following, the lower diffusion barrier of the Lander molecules plays also an important role in the manipulation experiments. To observe Lander molecules on the terraces it is necessary to cool the sample down to about 780 K before depositing the molecules, or to move them onto the terraces by lateral manipulation.

Several other types of Landers have recently been synthesized, with lengths varying between 17 and 30 Å [96] and some others are still in the design phase. In Fig. 16 two examples of other molecules of the Lander family are shown. The first one (Fig. 16(a)) is the so-called Reactive Lander and consists of the same four lateral spacer legs as in the case of the single Lander and a central board longer than

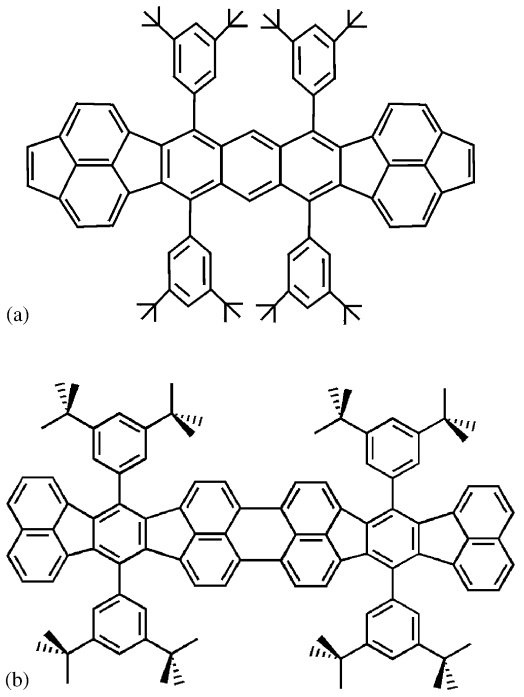

Fig. 16. Chemical structure of (a) a reactive Lander molecule showing a central board longer than for the single Lander and ending on both sides with double bonds, and (b) a L-Lander molecule. The distance between the front and the back legs is in this case designed to be larger than in the case of a simple Lander, resulting in a very small steric crowding.

for the single Lander and ending on both sides with double bonds. The second one is a long *L*-Lander (Fig. 16(b)), which has been recently investigated by STM at room temperature on Cu(1 0 0) [101] showing that, as in the case of the normal Lander, the molecule adapts itself to the surface by rotating the legs and decreasing the board-substrate distance. In that case, due to the larger distance between the spacer legs, a very small steric crowding takes place and a higher flexibility of the molecule is expected. Many different configurations for this molecule on a Cu(1 1 1) surface have been observed also by STM at low temperature [102]. On Cu(1 1 0), an oxygen induced surface reconstruction can be used to form periodic stripes of different controlled dimensions. It has been recently shown that Single Lander and Violet Lander molecules adsorb selectively in different orientations on these stripes, adapting to the dimensions of the template [103].

An even longer Lander, equipped with four legs on each side of the molecular wire, has been recently synthesized and investigated by STM at room temperature on a Cu(1 0 0) and on a nanostructured Cu(1 1 1) surface [104], showing that in that case, not only the legs are free to rotate, but also that the central board is distorted at double steps.

5. Investigation of large molecules by LT-STM: experimental solutions

The ability of LT-STM to perform controlled manipulation of single atoms and small molecules described above has been recently extended to the manipulation of complex molecules. Large molecules

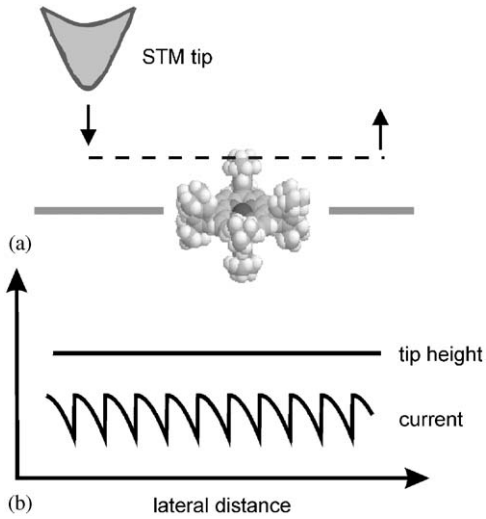

Fig. 17. Lateral manipulation in constant height mode: (a) schematic of the manipulation process, (b) sketch of the current signal recorded during the manipulation.

have been successfully manipulated at room temperature [10], but to obtain quantitative information about the details of the process, the stability and the low noise level achievable by LT-STM are necessary. The study of the feedback signal recorded during lateral manipulation, possible only at low temperature, is fundamental to understand the manipulation process itself and to study the internal mechanics of the molecule when it moves under the action of the tip. In the case of complex organic molecules, molecular flexure and reorientation of the internal conformation play an important role and one expects a different translational movement than in the case of atoms or simple molecules.

However, due to the complicated structure of the molecules and to their high conductance, using the traditional lateral manipulation mode it is not possible to move TBPP molecules on copper surfaces at low temperature. The main problem of the normal manipulation technique is that the feedback loop keeping the current constant is still active, so that the tip retracts when it approaches the molecule, giving rise, in case of complex molecules, to instabilities in the vertical position of the tip. To successfully manipulate large, complex molecules like TBPP and Lander some technical improvements of our experimental technique have been necessary.

To succeed in the lateral manipulation of TBPP at low temperature we developed a new mode of manipulation, the so-called “constant height manipulation mode” [105]. The idea is to keep the tip at a fixed distance from the surface when it is moved laterally across the molecule. Such a technique makes the interaction between tip and molecule stronger and provides the molecule enough energy to overcome the diffusion barrier. To keep the tip height constant, the feedback loop is switched off. The current signal can then be recorded and contains the information about the mechanism of the manipulation process.

The principle of the lateral manipulation in constant height mode is shown in Fig. 17. A first scan in constant current mode over the molecule is necessary to determine the local angle of inclination of the surface. Then the feedback loop is switched off and the height of the tip decreased by a selected amount Δz. The tip then moves along the chosen manipulation path (Fig. 17(a)) and both tip height and current

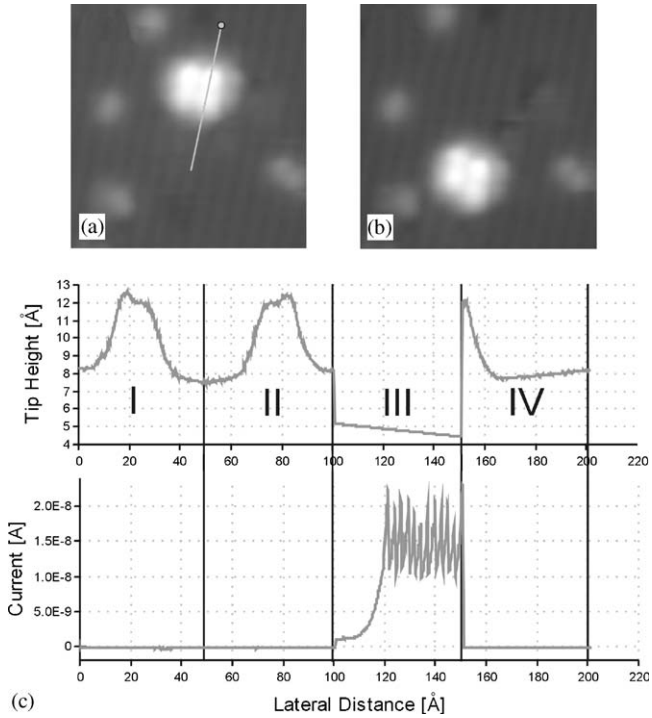

Fig. 18. Manipulation in constant height mode of a Lander on Cu(2 1 1) along the board direction. (a) STM image of the molecule before manipulation. The line indicates the manipulation path followed by the tip, and the small circle the starting position. (b) STM image of the molecule after the manipulation. As one can see the molecule has been pushed along the intrinsic steps without changing its orientation, but changing the conformation of the legs. (c) Tip height curves and tunneling current recorded during the complete process of manipulation. The manipulation is performed by reducing the height of the tip by 3 Å and applying a voltage of 30 mV.

signal are recorded (Fig. 17(b)). The tip height signal remains in this case constant, while the information about the details of the manipulation process are now shown by the tunneling current signal.

Fig. 18 shows an example of manipulation in constant height mode, as it appears on the computer screen in real time. A Lander molecule deposited on Cu(2 1 1) is imaged in Fig. 18(a). The initial and final points of the desired lateral manipulation are chosen and indicated by a line starting with a small circle, as shown in Fig. 18(a). The chosen manipulation parameters (tip height, velocity, and tunnel voltage) are set manually before the process starts. The result of the manipulation is then visualized (Fig. 18(c)). The upper curve shows the tip height signal. In the curve it is possible to distinguish four parts. The first two reflect the tunneling of the tip forward and backward over the molecule in constant current mode, the third part shows the manipulation at lowered constant height.

The forth and last part of the curve shows the final tunneling sweep in constant current mode along the manipulation path in the backward direction. It is important to note that by comparing this fourth signal with the second one it is possible to see whether the molecule has been moved or modifications in the tip form have occurred during manipulation. The lower curve shows the tunneling current recorded during the process. As one can see, the current remains constant in parts I, II and IV, while it shows

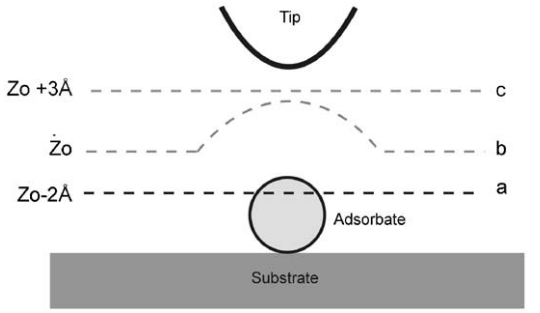

Fig. 19. Schematic comparison between manipulation in constant height mode (curve a), imaging in constant current mode (curve b) and imaging in constant height mode (curve c). Z_0 is the tip–surface initial distance as determined by the tunneling parameters in constant current mode.

the expected periodic manipulation signal in part III. The STM image recorded after the manipulation (Fig. 18(b)) shows the final position of the molecule.

The described procedure is quite versatile and can be applied with small modifications to many other situations. For example, a manipulation with extension has been developed, which allows to fix the two reference points and to extend the manipulation length by a chosen amount. The method is especially helpful for removing a molecule from a step edge bringing it to the free lower terrace or (by applying an extension in the opposite direction) to move a large molecule by pulling at a chosen internal part, like for example a single leg.

Moreover, the method developed for lateral manipulation has been extended to imaging the molecule in constant height mode. Fig. 19 schematically compares the typical movements of the tip for scanning in constant current mode (curve b), manipulating in constant height mode (curve a), and imaging in constant height mode (curve c). A plane subtraction to take into account the inclination of the surface during the scanning is done similarly as during manipulation. Imaging complex molecules in constant height mode has the advantage that the oscillations of the tip due to the feedback loop are avoided and a much clearer and more detailed image is recorded [106]. Moreover, the interaction between tip and molecule can be investigated in detail.

In Fig. 20 an image of a TBPP molecule on Cu(1 0 0) recorded in constant current mode is compared with some examples taken in constant height mode for different decreasing tip heights. In the case of TBPP and Lander, the STM images recorded for different values and polarity of the tunneling bias voltage do not show any dependence on the tunneling parameters. However, a dependence of the images on the tip–surface distance is observed, showing that a strong tip–molecule interaction takes place as soon as the tip gets in contact with the molecule. It is important to note that even if the apparent height of the molecule on Cu(1 0 0) is about 4 Å, its real height is about 8–9 Å. For this reason, a tip–substrate separation smaller than 8 Å means a direct contact between tip and molecule. By further decreasing the height of the tip, details of the conformations of the legs become visible. Under the action of the tip, the legs probably oscillate around their σ-bond showing a progressive enlargement of their image (Fig. 20(c) and (d)). Moreover, at still smaller tip height the pressure of the tip on the molecule is so large that details of the central ring become visible.

Constant height images show a high spatial resolution, which allows to distinguish details that are not visible in constant current images. This resolution is due to the elimination of the feedback loop

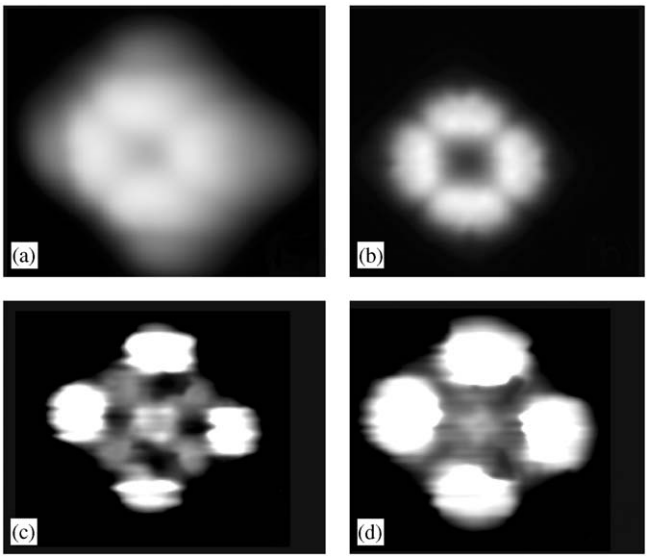

Fig. 20. (a) STM image in constant current mode ($V = 300$ mV, $I = 400$ pA) of a TBPP adsorbed on Cu(1 0 0), compared with a sequence of constant height images of the same molecule recorded for different values of the tip–substrate distance: (b) 8 Å, (c) 5 Å, and (d) 4 Å.

oscillations and of any discontinuous dependence of the tunneling current from the distance that take place during the scan in constant current mode. Additionally, a strong effect of the mechanical pushing of the tip against the molecule is evident, allowing a detailed study of the interaction between tip and molecule.

6. Theoretical models and calculations

The theoretical method used in the present work to calculate STM images of molecular adsorbates is based on the electron scattering quantum chemistry (ESQC) method, developed by Sautet and Joachim [107]. This method provides a reliable solution to the complex problem of predicting how an STM image of a molecular adsorbate appears on the surface of a conducting substrate.

Different theoretical approaches to this problem have been presented within the last years, without however really solving the point. One initial trend was to calculate the electron-density maps of some molecular orbitals of the adsorbate and to compare them with the experimental STM image [108,109]. However, this comparison often gives contradictory results, since molecular orbitals are usually calculated on an isolated molecule. More sophisticated models use either the Tersoff Hamann approximation, valid however only for large tip–molecule separation [69,110], or more generally the Bardeen approach [111], modeling the surface by the comparatively simplified jellium model [112,113].

In ESQC [107,114], a different approach is used and the tunneling current is calculated taking into account the full geometry of tip, adsorbate, and substrate. The electronic structure of the complete system (tip, adsorbate, and substrate) is exactly calculated, determining a scattering matrix, which is used to evaluate the tunneling current. The substrate is described atom by atom and restricted to a finite number

of surface atoms, while periodic boundary conditions are used to get the band structure of tip and surface. ESQC models the STM tunneling gap as a periodic substrate, a single adsorbate and a periodic tip. The system is considered symmetric. Tip and surface are modeled by the same number of atoms and are necessarily made of the same element. For each position of the tip apex on the molecule, several hundred molecular orbitals are used to describe the electronic properties of the tip–molecule–substrate system. The surface atoms and the organic molecule are described taking into account all valence molecular orbitals.

Bouju et al. [115] have recently developed a computer program which realistically simulates the function of an STM. The program takes into account the complete van der Waals forces between tip, manipulated atom, and surface, while the tunneling current is calculated by ESQC. Finally, the program reproduces the mechanics of the microscope, taking into account also the feedback effects. This program realizes a "virtual STM", able to reproduce the functions of a real STM and to virtually manipulate single atoms and small molecules.

To apply the method developed in the "virtual STM" to the case of large molecules, the calculations should also take into account internal changes of the configuration under the action of the tip. To calculate such configurations by quantum chemistry or molecular dynamics methods requires a too long calculation time. For this reason, the deformation of the molecule on the surface and under the action of the tip is presently calculated by molecular mechanics (MM), a standard method of modeling a molecular geometry using Newtonian mechanics. In this method, the total energy of a system is described by an empirical analytical function of the coordinates of its constituent atoms and the geometry of the system is optimized by minimizing this energy. MM is combined with ESQC to optimize the geometry of the adsorbate for each point of the image and to calculate the mechanical interaction between the adsorbate and the tip.

The molecule is initially placed above the surface in the conformation adopted in the gas phase (as determined by standard X-ray diffraction methods in the gas phase). The distance between molecule and surface is then decreased. Van der Waals forces attract each atom of the molecule toward the surface and deform the molecular configuration. At each step, the equilibrium configuration is calculated by molecular mechanics. The same kind of procedure is applied when the tip approaches the molecule: the tip attracts the atoms of the molecule and deforms its chemical bonds. For each position of the tip the configuration is optimized by MM and the corresponding tunneling current calculated by ESQC. As one can see in the example reported in Fig. 21, the calculated STM image of a molecule can be obtained and its precise configuration on the surface extracted.

The described procedure is useful not only for the interpretation of STM images, but also to understand the transition between different images and to describe the time evolution of the molecule, for example during a manipulation process.

In any STM experiment there is an intrinsic contradiction, because the action of the tip locally modifies the system when it records the information (i.e. tunneling current). Moreover, as the configuration of the molecule changes under the action of the tip, the current measured with the same tip on a single atom of the molecule varies. It is therefore necessary to have a theoretical tool, like the described "virtual STM", able to perform the opposite way, extracting the configuration changes from manipulation curves and STM images.

The MM-ESQC method was shown to be successful in modeling molecular images and manipulation curves. Important details on the internal configuration changes of molecules during their lateral manipulation have been extracted from the experimentally recorded manipulation curves, as discussed in detail in the following sections. Moreover, the method can be used not only to extract information from experimental data, but also to predict the behavior of a molecule on a surface, becoming a

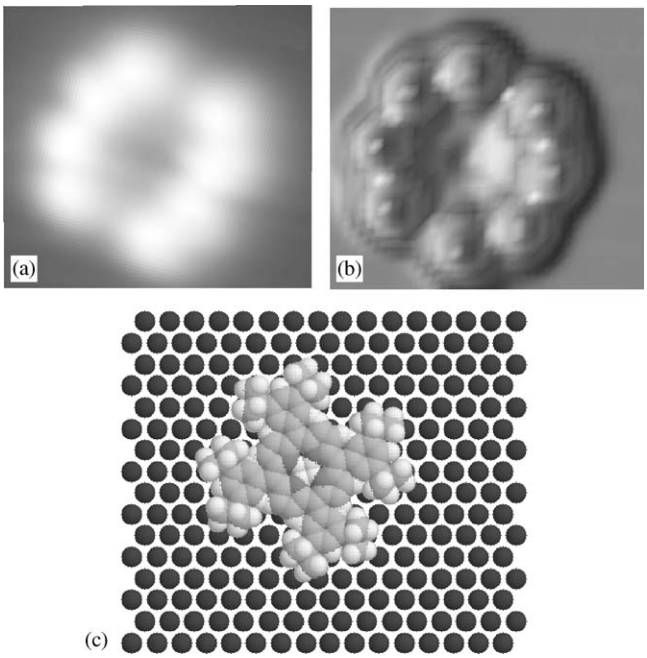

Fig. 21. (a) Experimental and (b) calculated STM images of a TBPP molecule on Cu(1 1 1). (c) Sphere model used for the calculation, showing the orientation of the molecule, as obtained from molecular mechanics optimization.

fundamental tool for the design of new molecules, capable of performing special movements under the action of an STM tip and acting like individual nanoscale molecular machines. For example, the movement of a kind of "molecular barrow" has been theoretically calculated. Its geometry and composition have been optimized with the aim of obtaining large internal configurational changes by STM manipulation [116]. Such molecule, schematically shown in the sphere model of Fig. 22, has been recently synthesized [117] and it is presently investigated by LT-STM, to record the manipulation signal and identify the signature of the wheels movement. The molecular wheelbarrow consists of two TBP-legs and two wheels (ethynyl triptycene groups) connected to a polycyclic aromatic hydrocarbon platform.

7. The principle of a molecular switch realized by manipulation

Molecular switches are common and important functional elements in nature: Many biological systems are based on the combined work of single large molecular units, where the different functions are realized by means of conformational changes. The study of the switching processes in molecules is especially interesting for the development of new technologies, and molecular switches could be integrated in artificial nanostructures and find application in nanoelectronics [118]. The study of the properties of molecular switches is for these reasons a very promising research field. The possibility to address adsorbed molecules by STM and to directly measure their switching behavior has succeeded in a few cases and a reversible change in the tunnel current through the molecule has been directly measured. Such investigations are important to understand the mechanisms that cause conductance switching in

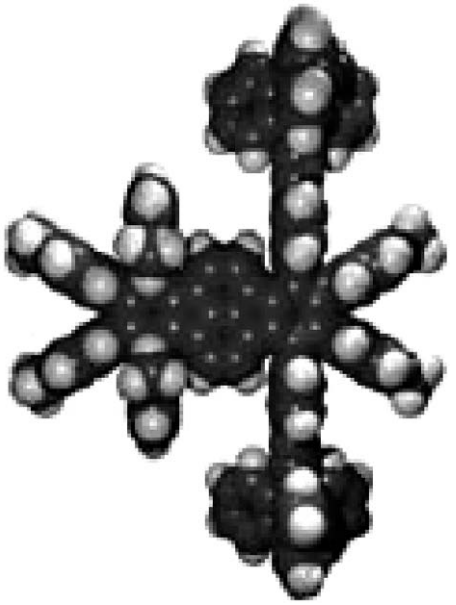

Fig. 22. Sphere model of a molecular wheelbarrow.

single molecules. Recently, the electronic characteristics of mechanical [119] and electro-mechanical [11] molecular switches have been measured and field-effect-based [120] molecular switches have been theoretically investigated. Moreover, a solid state, electronically addressable, switching device has been fabricated by means of a single layer of bistable molecules [121,122] and stochastic on–off switching was observed in simple wired molecules [123].

The manipulation at low temperature of a single TBPP molecule offers the opportunity to investigate in detail the mechanical-induced switching processes of single molecules. We have recently demonstrated that the STM-tip can be used to induce a conformational change in a single TBPP molecule, and that this alters the electronic properties of the tunnel junction [124]. In other words, a conformational molecular switch can be realized by rotating a single lateral group of the molecule in and out of the porphyrin plane. Such a rotation is made possible by lateral and vertical manipulation, modifying in a controlled way the internal conformation of the molecule.

The idea of the experiment is sketched in Fig. 23: if we could place one of the lateral TBP-groups of a TBPP molecule between two electrodes and apply a small voltage across it, it would then be possible to vary the current through the circuit by rotating the TBP-group, yielding either a high or a low resistance of the junction. Calculations show that in the case of TBPP molecules the resistance would change by many orders of magnitude by a 90° rotation of a leg of the molecule. To implement the molecular switch in a real environment, TBPP molecules deposited on the stepped Cu(2 1 1) surface were investigated. The role of the two electrodes was played on one side by the metallic surface and on the other by the STM tip.

As already mentioned in Section 4 and as shown in the STM images of Fig. 24, TBPP molecules on Cu(2 1 1) normally show eight lobes, with an apparent height of 2 Å (Fig. 24(a)), corresponding to four legs oriented nearly flat on the surface [94]. In a few cases, a single brighter lobe appears among the

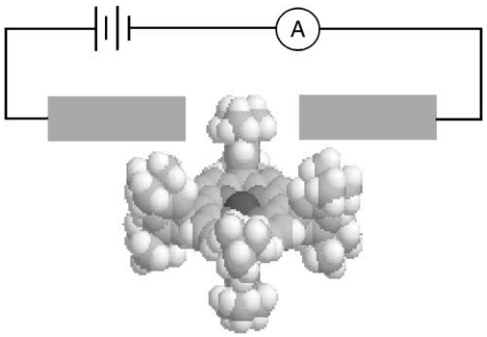

Fig. 23. Model of a molecular switch consisting of a single TBPP molecule. The tunneling current passes through one leg and the conductivity depends on the leg conformation. Reprinted with permission from Ref. [124]. Copyright 2001 by the American Physical Society.

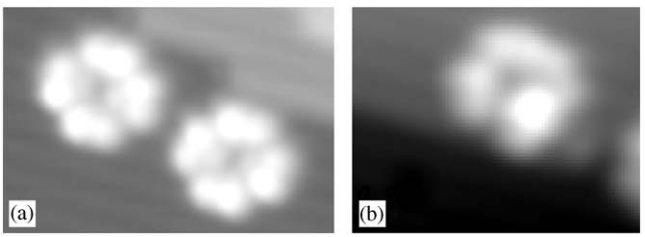

Fig. 24. (a) STM image of two TBPP molecules deposited on Cu(2 1 1) lying flat on the surface. (b) STM image of a TBPP molecule on Cu(2 1 1) showing one leg rotated out of the plane of the porphyrin. Reprinted with permission from Ref. [124]. Copyright 2001 by the American Physical Society.

double lobes with an apparent height of about 4 Å, indicating that one leg is rotated nearly perpendicular to the plane of the substrate (Fig. 24(b)). This peculiar conformations are imposed to the molecule from the (1 1 1) facets of the stepped Cu(2 1 1) surface.

MM-ESQC calculations, taking into account a total of 770 molecular orbitals, have been performed to determine the tilt angle of the legs for both configurations, finding for the case of flat legs (Fig. 25(a)) an angle of 10° relative to the surface, while in the case of Fig. 25(b) one leg is rotated by 55°. The corresponding calculated STM images are reported in Fig. 25(a) and (b), while molecular models (Fig. 25(c) and (d)) roughly visualize the two different conformations of the molecule. It is important to note that the calculated tunneling resistance through a leg decreases more than one order of magnitude when the lateral group changes its conformation from the flat case of Fig. 25(a) to the rotated case of Fig. 25(b). Therefore the flat leg configuration can be called the “OFF-state” of the switch, while the rotated leg can be considered the “ON-state”.

A further step toward the implementation of the molecular switch is to use manipulation techniques to reversibly modify the molecular conformation. First of all we have applied the lateral manipulation methods to the TBPP molecule, without however allowing the molecule to move. Passing with the tip over the molecule in lateral manipulation condition induces a rotation of legs out and/or in the porphyrin plane. Fig. 26 shows a series of these manipulations, where one leg of the molecule is reversibly rotated in both directions.

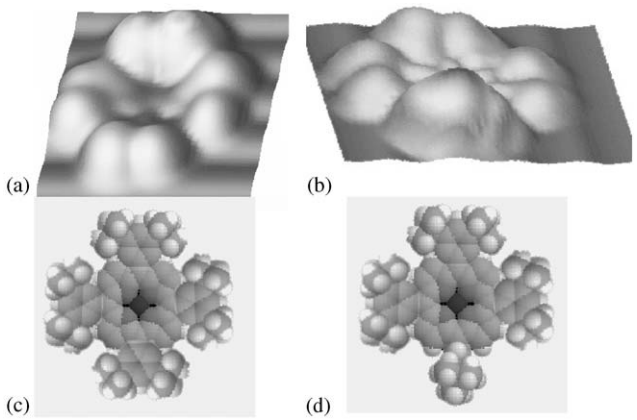

Fig. 25. Calculated full STM images of a TBPP molecule on Cu(2 1 1) corresponding to the flat conformation (a) and to the rotated leg case (b). The molecule orientation and its intramolecular conformation have been obtained using ESQC and optimized to minimize both the potential energy of the molecule and the numerical distance between the experimental and calculated images. (c) and (d) sketch of the approximate molecular conformation for (a) and (b). Reprinted with permission from Ref. [124]. Copyright 2001 by the American Physical Society.

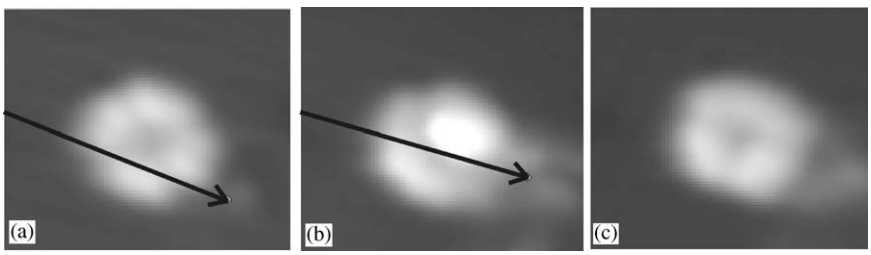

Fig. 26. STM images showing the rotation of a leg induced by lateral manipulation. The manipulation was performed in the direction indicated by the arrows at a tunneling resistance of $6 \times 10^4\,\Omega$. The image in (b) shows the result of the manipulation performed in (a) and the one in (c) the result of the manipulation in (b). Reprinted with permission from Ref. [124]. Copyright 2001 by the American Physical Society.

The rotation of a single leg from the rotated to the flat conformation, i.e. from the ON to the OFF state of the switch, is possible also by vertical manipulation. The vertical manipulation was performed by positioning the tip above the leg and reducing the tip–surface distance, thus pushing the leg downwards. After this manipulation sequence, the leg adopts the 10° conformation angle showing its characteristic two lobes. An example of this manipulation process is reported in Fig. 27.

To demonstrate the principle of the molecular switch, we have quantitatively investigated the interaction between tip apex and leg during a vertical manipulation sequence. In particular, we have measured the current passing through a single leg in real time during its rotation, applying a method normally used to measure barrier height and tip–surface interaction [125,126]. We are in this way able to demonstrate that the tunneling current through one leg strongly depends on the extent of its rotation.

A current curve recorded during the switching process is shown in Fig. 28. The tunneling current $I(z - z_0)$ is reported versus the height z of the tip on the surface. On a flat leg (switch OFF) the measured

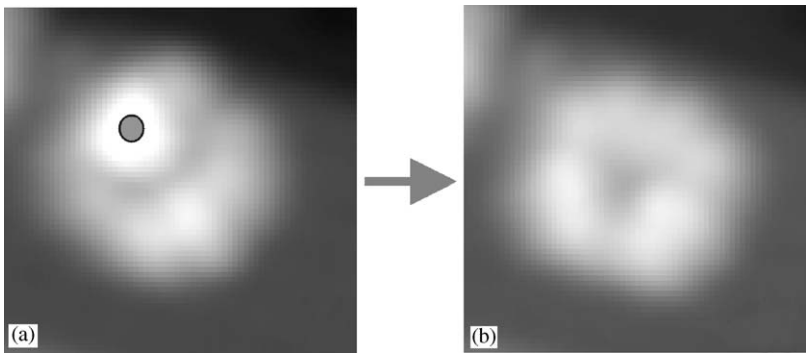

Fig. 27. STM images showing the rotation of a leg induced by vertical manipulation. (b) Result of the vertical manipulation performed by positioning the tip on the point indicated with a circle on the image (a). Reprinted with permission from Ref. [124]. Copyright 2001 by the American Physical Society.

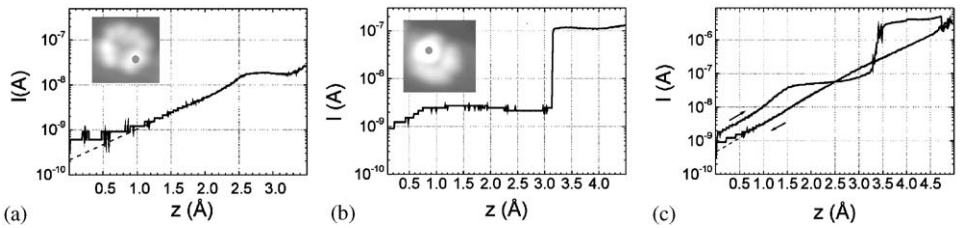

Fig. 28. $I(z)$ curves recorded (a) on an OFF-leg and (b) on an ON-leg. The exact position of the tip is shown in the insets. The starting tip–surface distance z_0 is respectively (a) 5.5 Å and (b) 7.5 Å, relative to the electrical contact point between tip and surface (12.7 kΩ STM junction resistance). (c) $I(z)$ curve recorded during the controlled rotation of a leg from the ON-leg to the OFF-leg states with $z_0 = 7$ Å. A sample voltage of 1 V has been applied during this $I(z)$ cycle. The dotted lines in (a) and (c) show the prolongation of the $I(z)$ behavior at low z, not visible in the experimental curves because of the limited sensitivity of the preamplifier. Reprinted with permission from Ref. [124]. Copyright 2001 by the American Physical Society.

$I(z)$ curve is shown in Fig. 28(a). Initially, the current grows exponentially as expected. A plateau occurs when the tip apex reaches the van der Waals contact point with the flat leg. Then the leg continues to be pressed by the tip, remaining in a planar conformation. The plateau in the current is well reproduced by model calculations and can be explained by the combined effect of the reorganization of the molecular orbitals and the geometrical deformation of the molecule. The current-height curve recorded on a rotated leg (switch ON) is shown in Fig. 28(b). In this case, the curve shows two plateaus, with a sudden change between them at $z = 3$ Å. The lower plateau is due to a competition between the reorganization of the molecular orbitals and the deformation of the molecule, which take place when the tip tilts the leg. The second one is due to the further pression of the tip on the flat leg. A third case, reported in Fig. 28(c), shows the $I(z)$ curve recorded during a complete ON–OFF cycle of the molecular switch. As one can see, after the rotation, the leg remains flat when the tip is retracted. A factor 10 in current is measured between the ON and OFF configuration at $z \sim 0$.

Molecular mechanics calculations show that a leg rotation of 90° can induce a change in resistance of over six orders of magnitude, while in our experimental condition the value of one order of magnitude is

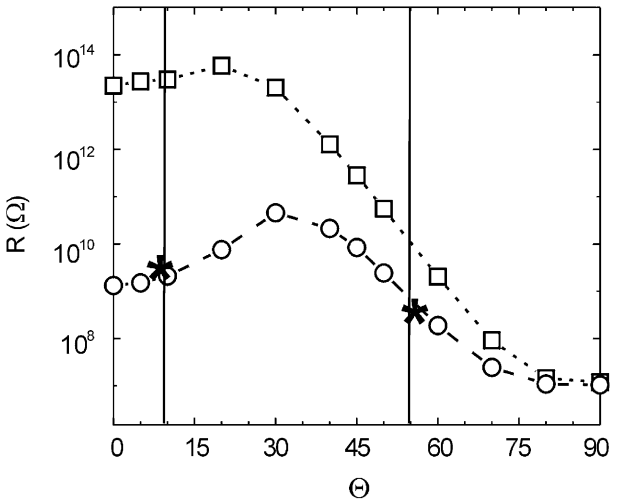

Fig. 29. Calculated variation of the tunnel resistance (R) for the molecular switch given by the rotation of a leg of a TBPP vs. the rotational angle Θ of one leg, as obtained by ESQC. Two different tip apex to surface distances are reported: $z_0 = 7$ Å (circles) and $z_0 = 9$ Å (squares). The vertical lines indicate the experimental values of the rotational angles and the stars indicate the two experimental points.

reproduced, as shown in the calculated curves for the resistance as a function of the rotational angle of the leg reported in Fig. 29. The calculations show that a z_0 value of 9 Å would provide a better difference between the ON and the OFF states. However the tunneling current in the OFF state at this distance is too low to be measured, so that the experimental values have been taken at $z_0 = 7$ Å.

Very recently, the switching energy required to operate such a molecular switch has been measured using a noncontact atomic force microscope [127], showing that the rotation of the leg requires an energy less than 100×10^{-21} J, which is four orders of magnitude lower than state of the art field effect transistors.

In conclusion, the reported experiments show that the controlled rotation of a leg of a TBPP molecule can be performed by LT-STM by applying the techniques developed for the manipulation of single atoms, giving the opportunity of realizing the principle of a conformational molecular switch.

8. Study of the intramolecular mechanics of TBPP manipulated on Cu(1 0 0)

In this section we will show how it is possible to apply the technique of lateral manipulation at constant height to investigate the internal mechanics of a TBPP molecule. The aim is here to induced motion and deformation of a part of the molecule on a Cu(1 0 0) surface in a controlled manner, monitoring it in real time [128]. This experiment represents the first step toward the realization of a molecular nano-machine, where a physical link between the molecule and the STM tip apex can be established by their direct electronic interaction.

A molecular machine can be defined as a molecule designed to do a computation, a motion or a measurement by itself [116]. The molecule performs such a task responding to a data input or command coming from an operator. The operator observes the realization of the task directly on the molecule at

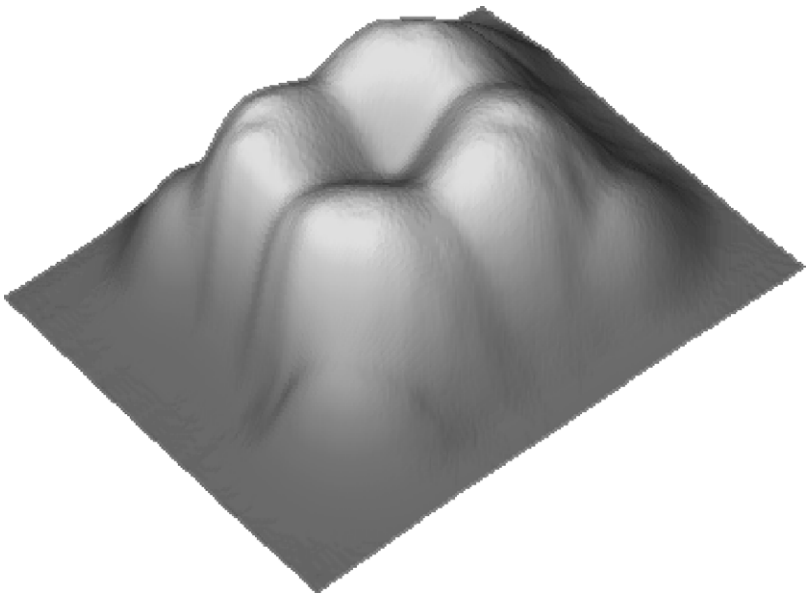

Fig. 30. STM image (in 3D) in constant current mode of a single TBPP molecule adsorbed on Cu(1 0 0). Reprinted with permission from Ref. [128]. Copyright 2001 by the American Physical Society.

the end of the operation cycle. To implement a nano-machine under the action of an STM tip, special molecules, designed to be moved on a surface by the tip of an STM should be used, where the movement of internal part could be clearly recorded by measuring the manipulation curves.

A sub-monolayer amount of TBPP molecules was deposited onto a Cu(1 0 0) surface. In the STM image shown in Fig. 30, a TBPP shows four bright lobes with some lateral residual echoes due to the orientation of the lateral groups, while the porphyrin ring is hardly visible. Calculations of the STM image show that each lobe corresponds to a leg oriented nearly perpendicular to the surface, at an angle of about 80° [94].

The manipulation experiment has been performed in constant height mode [105]. The height of the tip on the surface was reduced step by step and the manipulation was performed at the height at which the molecule starts to move. The tunneling current was recorded over the TBPP molecules for different altitudes, by passing across it with the tip in constant height mode before the molecule starts to move. The corresponding curves are shown in Fig. 31. As one can see, up to height of about 9 Å the molecule do not move and a maximum tunneling current of about 2×10^{-8} A is measured.

In order to manipulate the TBPP we have chosen a pushing mode performed on a single leg, as shown in the manipulation sequence reported in Fig. 32. The arrow shows the exact path followed by the tip. The height of the tip on the surface is in this case 9.6 Å and an average tunnel current of about 10^{-6} A is measured.

The current curve $I(x)$ recorded during the manipulation is presented in Fig. 33. The sequence reflects first of all the Cu(1 0 0) lattice periodicity. However, details in each period do not resemble the regular sawtooth signals recorded during STM manipulations of atoms and diatomic molecules (see Fig. 7). Magnified parts of the signal show a specific intra-period signature, peculiar of this specific type of manipulation.

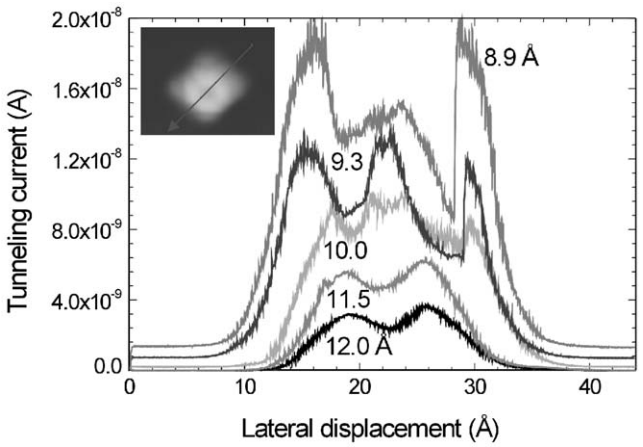

Fig. 31. Constant height $I(x)$ tunneling current intensity recorded over a TBPP molecule at different altitudes. The tip apex approaches over the center of the molecule, at a bias voltage $V = -50\,\mathrm{mV}$. The tip–surface distance, z, is defined by the center-to-center distance between surface and tip atoms at the electrical point contact. The experimental tip–surface separation at the electrical point contact corresponds to $z = 4\,\text{Å}$. The exact path of the tip is shown in the inset. The tip–molecule distance is kept large enough to avoid the manipulation of the molecule. Reprinted with permission from Ref. [128]. Copyright 2001 by the American Physical Society.

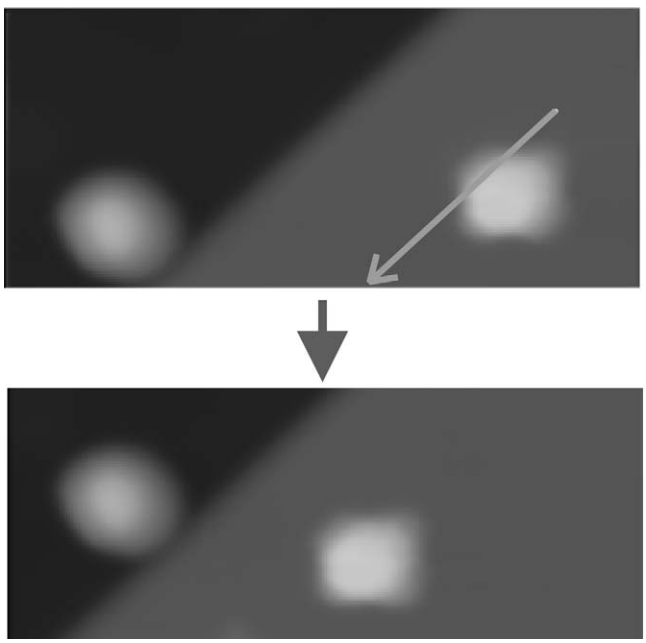

Fig. 32. STM images of a TBPP on Cu(1 0 0) recorded before and after the manipulation process, when the molecule is pushed along a single leg. The arrow on the top image indicates the exact path followed by the tip.

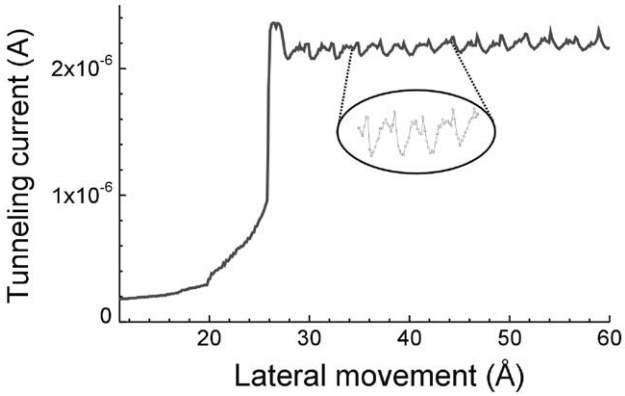

Fig. 33. Experimental current curve recorded during the manipulation of a TBPP on Cu(1 0 0) as shown in Fig. 32. The inset shows details of the signal.

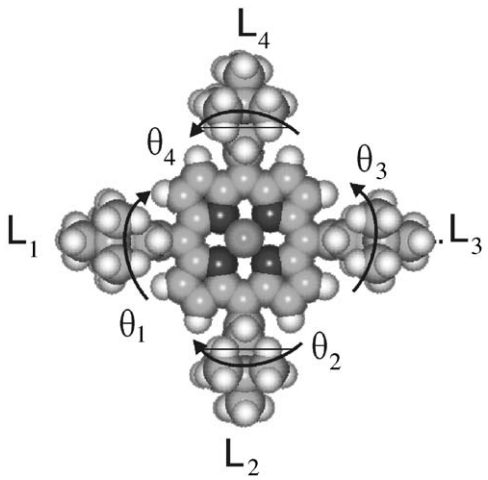

Fig. 34. Nomenclature assigned to legs and angles. Rotation axes are defined relative to 90° for a leg perpendicular to the surface.

Details of the intramolecular mechanics occurring during a manipulation sequence have been extracted from this manipulation curve by ESQC and molecular mechanics calculations. We denote legs and angles as shown in Fig. 34, where L_1 is the leg pushed by the tip and a rotational angle of 90° corresponds to a leg perpendicular to the surface. We found, (Fig. 35), that the main contribution to the signal comes from the leg L_1, which directly interacts with the tip apex. However, the leg in front of the tip (L_3) contributes to the recorded signal too. The movements of the two legs are very small, oscillating them by only a few tenth degrees. However, such a very sensitive analysis demonstrates that detailed "on line" information on the internal mechanics of a molecule can be extracted from $I(x)$.

Finally, we considered how the manipulation signal $I(x)$ results from the superposition of four tunnel paths, one per leg, and how the deformation of L_3 contributes to $I(x)$. The idea is schematically represented in Fig. 35(a). The central porphyrin ring acts as a wire connecting electronically L_3 to the tip apex and

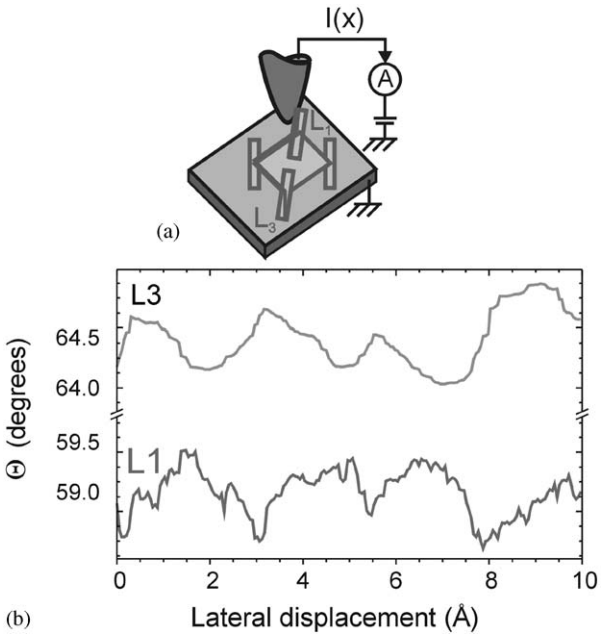

Fig. 35. (a) Schematic representation of the lateral manipulation process. (b) Characteristic conformational angles for L_1 and L_3 during the manipulation, as extracted from the experimental manipulation signal. Reprinted with permission from Ref. [128]. Copyright 2001 by the American Physical Society.

reporting about the L_3 motion during a manipulation sequence. The very small contribution of L_3 to the total manipulation current could be extracted [128].

Substituting the porphyrin by a better molecular wire will maybe improve the tunneling wiring effect and will allow to experimentally record a more intense signal. The manipulation of a molecule equipped with wheels (instead of legs) or arms and consisting of a molecular wire as central body (to interconnect the moving parts of the molecule to the tip apex) is the next step toward the design of molecular wired nano-machines.

9. Selective adsorption and surface restructuring induced by a Lander molecule

The experiment described in Section 8 has shown the lateral manipulation of single TBPP molecules and the extraction of the intramolecular mechanical movement of the molecule during the manipulation, leading to the conclusion that the internal movement of the TBPP is quite small, rotating the legs only of a few tenth degrees. To go a first step further in the direction of realizing a molecular nano-machine, new molecules should be found, showing more pronounced conformational changes during the manipulation or a more conducting central body, which can allow to transmit a stronger manipulation signal. In this respect, the Lander molecule is a very interesting model system, because it is formed by a central conjugated polyaromatic molecular wire separated from a metallic surface by four spacer groups. As already discussed in Section 4, the spacer groups of the Lander are the same TBP-legs as in the case of the TBPP molecule. The Lander was specially designed to investigate molecular wires, electrically decoupled through the four lateral groups, on metallic surfaces [96].

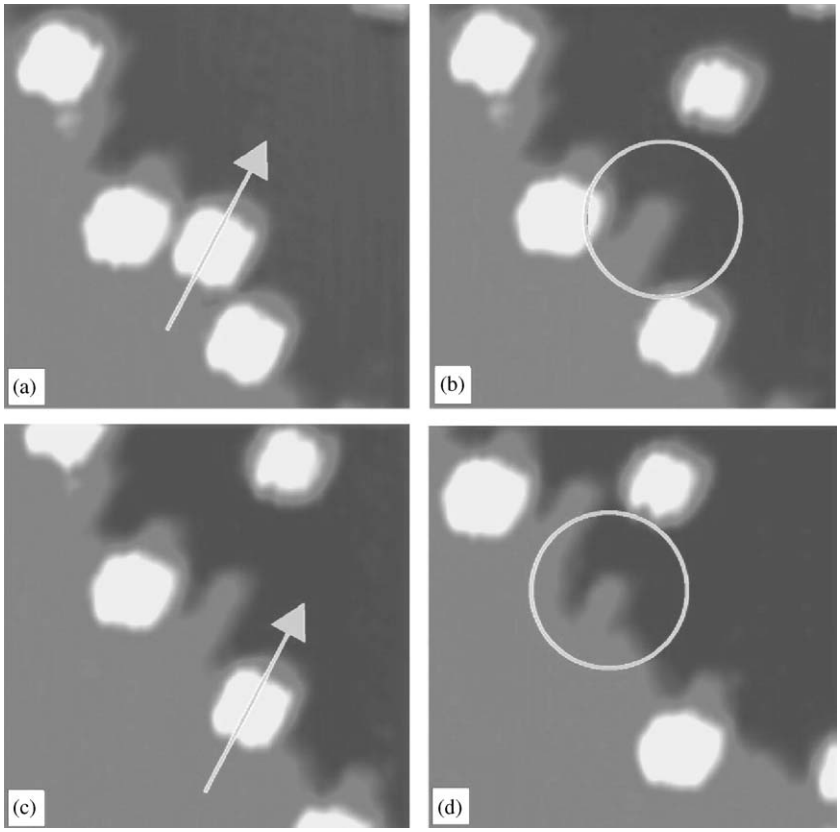

Fig. 36. (a)–(d) Manipulation sequence of the Lander molecules from a step edge on Cu(1 1 0). The arrows show which molecule is being pushed aside; the circles mark the tooth-like structures that are visible on the step where the molecule was docked. All image dimensions are 13 nm by 13 nm. Reprinted with permission from Ref. [98]. Copyright 2001 AAAS.

When a large molecule adsorbs on metal surfaces, its interaction with the substrate can be quite complex and can reveal new and unexpected physical properties, which are difficult to predict from investigations in the gas phase. A complex molecule can adapt itself to the substrate changing its internal conformation, as we have seen in the case of TBPP [94,124], but it can also in same cases induce a restructuring of the surface accompanied by mass transport in order to maximize its adsorption energy [129,130].

The adsorption of Lander molecules on Cu(1 1 0) has been recently studied by Rosei et al. [98]. They found that the molecule acts as a template, restructuring the surface at the step edges and forming metallic nanostructures that are adapted to the dimension of the molecule. Upon submonolayer deposition of the Lander at room temperature, the molecules diffuse to the step edges. As one can see in Fig. 36, after removing a molecule by pushing it away with the STM tip, an underlying restructuring of the step edges induced by the molecule is revealed. The so obtained nanostructure has a width of two atomic copper rows and a length of about seven Cu atoms.

We have investigated the same system by STM at low temperature [131], in order to reveal details of the molecular conformations and to perform controlled manipulation of the molecule along the

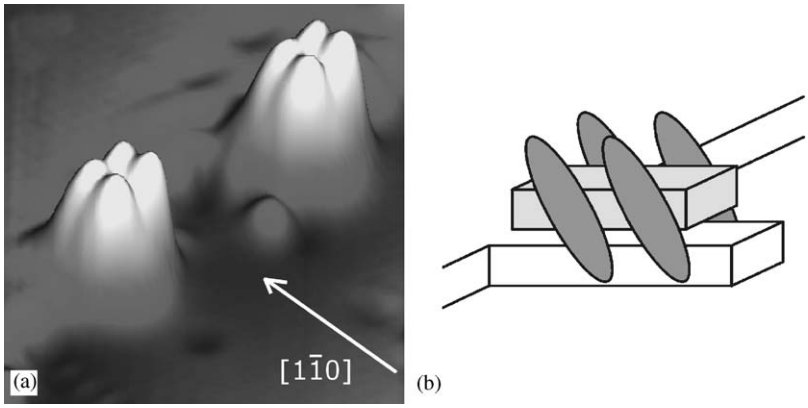

Fig. 37. (a) Three dimensional view of an experimental STM image of two Lander molecules adsorbed at a Cu(1 1 0) step edge. (b) Schematic model of the adsorption conformation. Reprinted with permission from Ref. [131]. Copyright 2004 by the American Physical Society.

nanostructure. In our case, annealing to 370 K was necessary to induce the surface restructuring efficiently. Different conformations of the Lander molecules on the rearranged atomic double rows could be resolved. Fig. 37(a) shows a STM image of a Lander molecule adsorbed at a step edge in the most frequently observed conformation, while in Fig. 37(b) a schematic model of this adsorption conformation is reported.

Conformational changes of the Lander molecule on the copper atomic wire have been induced by lateral manipulation with the STM tip. By moving the tip just a short path across the molecule in constant current mode at a tunnel resistance of about 100 kΩ, only the orientation of a pair of legs on one side of the central board changes while the entire molecule does not move. As we will discuss in better detail in Section 10, the lateral displacement of the entire molecule along the tooth can be obtained for a longer path and a lower tunnel resistance, up to a total removal of the molecule from the tooth. The different conformations of a single Lander molecule during a series of such STM leg manipulations are presented in Fig. 38. The changes in the orientation of the butyl-phenyl groups from image Fig. 38(a) to image Fig. 38(c) are clearly visible. This controlled manipulation permits to explore the two possible crossed legs conformations (Fig. 38(a) and (c)) and the parallel legs conformation (Fig. 38(b)) of this molecule. The molecular model of each conformation is shown for comparison. Note that the present parallel legs conformation is different from the initial position in Fig. 37(a): The legs are now rotated toward the lower terrace and the two lobes close to the step edge appear higher than the other two.

For a better understanding of the leg-induced conformational changes, the apparent lateral displacements of the single lobes during a full series of eight successive leg manipulations are plotted in Fig. 39. These lateral displacements are measured from STM images parallel to the central wire after selecting on the surface two fixed reference points (see scheme in Fig. 39). The position of the legs in Fig. 39(b) serves as a reference and corresponds to the central conformation IV. The curve is nearly periodic: in the even steps all distances are close to zero while in the odd steps two distances increase to about 2 Å and the other two remain fixed. The molecule flaps reversibly back and forth between the parallel conformation of Fig. 38(b) and one of the two crossed legs conformations (Fig. 38(a) and (c)). It is important to note that the position of two legs and therefore of the central board is always constant during these conformational changes, showing that the tip induces only a simple rotation of the legs without any translation of the

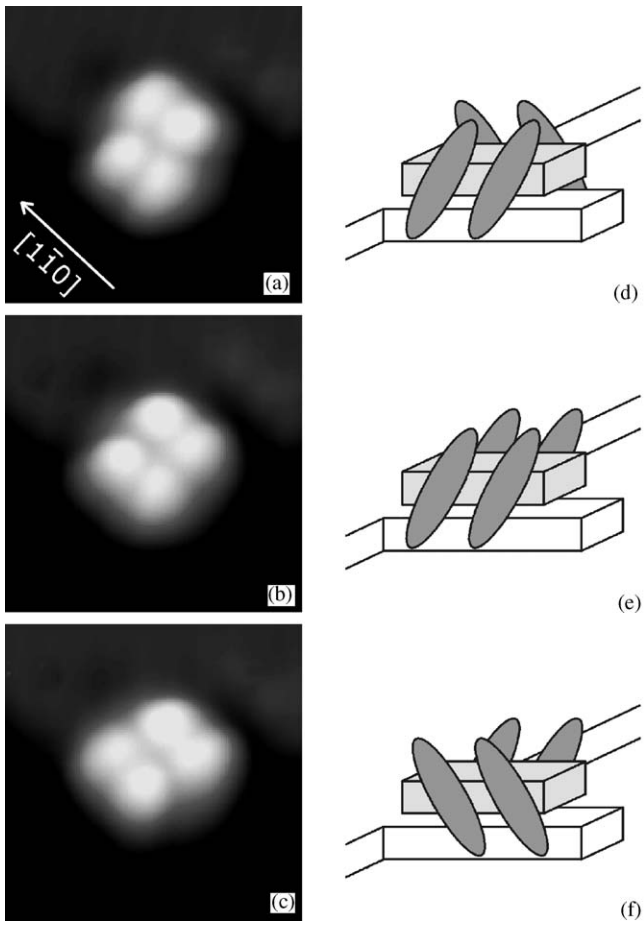

Fig. 38. Manipulation series of a Lander molecule adsorbed on a wire. (a)–(c) STM images ($45 \times 45\,\text{Å}^2$) of different conformations. (d)–(f) Schematic models of the corresponding molecular conformations. Reprinted with permission from Ref. [131]. Copyright 2004 by the American Physical Society.

whole molecule. Due to the strong steric coupling between the butyl-phenyl groups on the same side of the central wire, it is not possible to induce the rotation of one leg alone, as it was done for example with the TBPP molecule [124].

A different kind of selective adsorption and surface restructuring take place when the Lander molecules are deposited on Cu(2 1 1) [100]. An example of an STM image of Lander molecules deposited on Cu(2 1 1) has been already shown in Fig. 15. Because of the low diffusion barrier, the Landers had to be deposited at low temperature in order to find them uniformly distributed on the terraces. After evaporation at a sample temperature below 80 K most molecules are found isolated on the Cu(2 1 1) terraces without any preferential adsorption at high coordinated sites (i.e. step edges or defects), indicating that the diffusion of the Landers is suppressed below 80 K. Independently of the substrate [97–99], the molecules show the two different configurations already described in Section 4. On Cu(2 1 1) they are found oriented with the body parallel or perpendicular to the step edges and extending over three intrinsic steps.

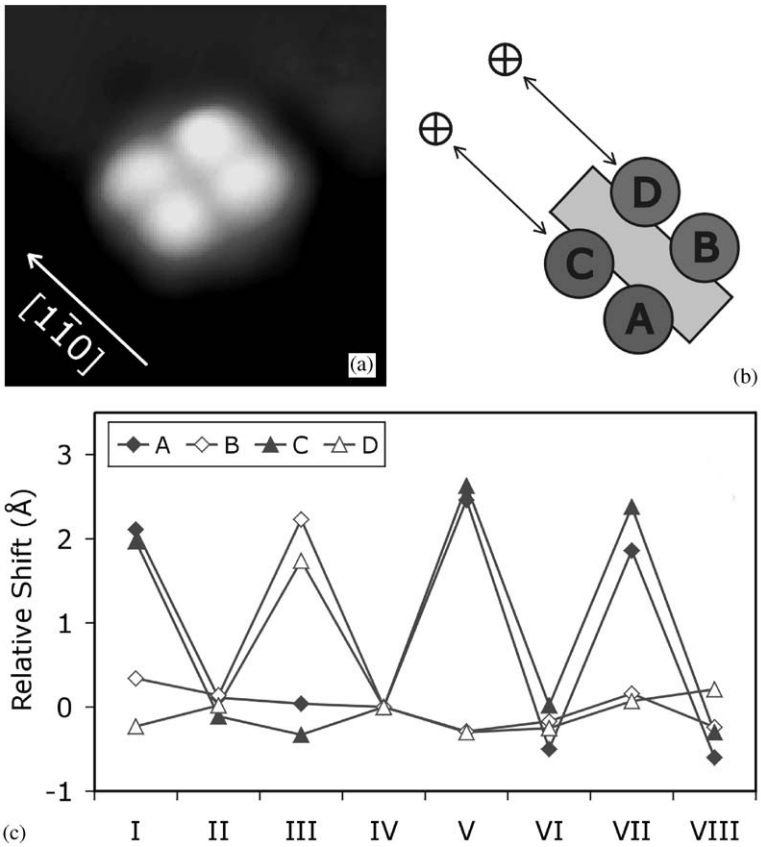

Fig. 39. Lateral shift of the four lobes of the Lander molecule during a manipulation series. (a) STM image of the initial position (45×45 Å^2). (b) Schematic view of the Lander molecule (where A–D denote the four lobes) and two reference points (crossed circles) on the surface, to which the distance from the legs is measured. The position of the legs is determined from linescans across the legs in [1 −1 0] direction, i.e. parallel to the two arrows. (c) Relative shift of the molecular legs A–D during the series. The roman numbers on the x-axis denote the different steps. Reprinted with permission from Ref. [131]. Copyright 2004 by the American Physical Society.

After evaporation at higher sample temperatures (between 160 and 330 K) the Lander molecules are always found at defect sites, usually at step edges, indicating that surface diffusion is not hindered. A typical overview scan after preparation at 330 K is shown in Fig. 40(a). As one can see, the molecules adsorb at [0 1 −1] directed terrace steps, furthermore exclusively at (3 1 1) steps and not at (1 1 1) steps. The board of the molecule is always aligned with the step edge whereas the internal conformation may again differ between crossed legs and parallel legs [97].

The (3 1 1) steps are restructured by the presence of Lander molecules. When the molecules are moved away from their adsorption site (Fig. 40(b)) by lateral manipulation, ditches on the lower side of the step edge become visible (Fig. 40(c)) proving that this surface restructuring is induced by the Lander molecules. The observation of restructured steps extending beyond the molecules (white arrows in Fig. 40(a)), visible prior to manipulation of the Landers, rules out that the reconstruction is only created by the STM manipulation.

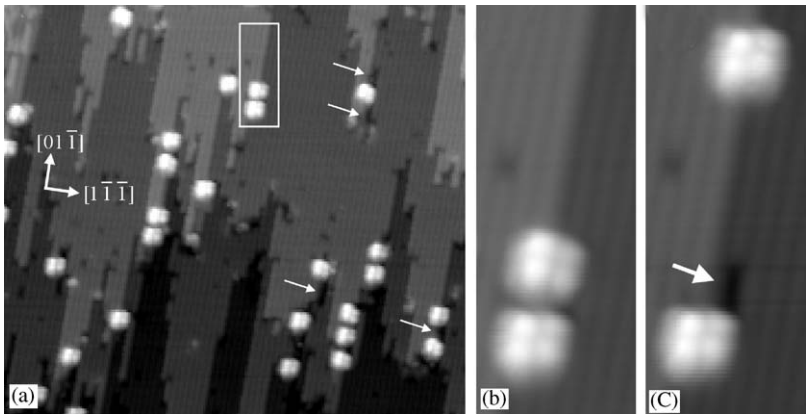

Fig. 40. Lander on Cu(2 1 1) after evaporation keeping the substrate at 330 K. (a) Overview (30×30 nm^2). All Lander molecules are adsorbed at restructured (3 1 1) steps. Arrows are pointing at restructured step edges in the vicinity of Lander molecules. The rectangle in (a) indicates the picture frame of (b) and (c) (4×10 nm^2). Between (b) and (c) one molecule has been moved along the step edge by STM manipulation, revealing the underlying surface restructuring. Reprinted from Ref. [100]. Copyright 2003, with permission from Elsevier.

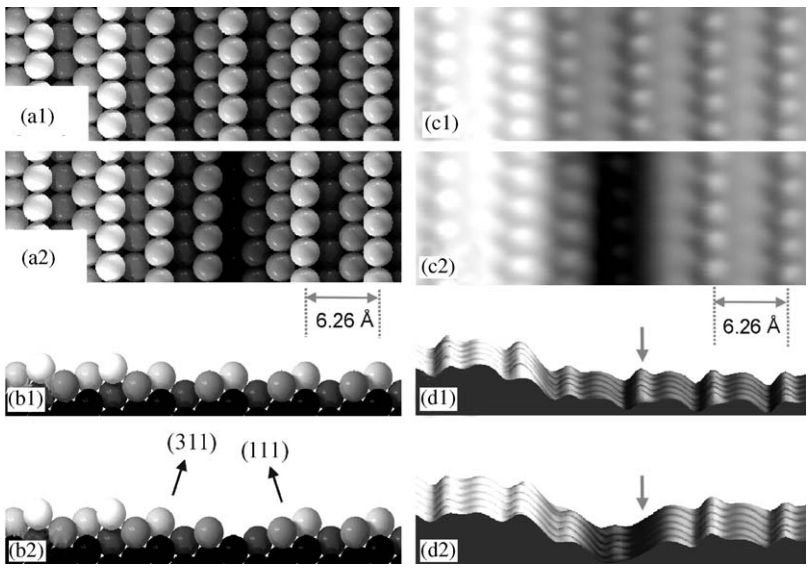

Fig. 41. Sphere models and STM measurements of a virgin and a restructured Cu(2 1 1) surface with a (3 1 1) step. The virgin surface is shown above the corresponding restructured one. (a) and (b): sphere models in top and side view, respectively. (c) STM image with atomic resolution of a virgin (c1) and a restructured (c2) step edge. (d) Pseudo three-dimensional STM images. The arrow in (d1) indicates the row that is missing in the case of restructuring (d2). Reprinted from Ref. [100]. Copyright 2003, with permission from Elsevier.

From STM measurements with atomic resolution as in Fig. 41(c) a model of the restructured surface (Fig. 41(a) and (b)) is deduced: At the bottom of a (3 1 1) step a closed packed row of adatoms is missing creating a (3 1 1) and a (1 1 1) micro facet. Thus the already existing (3 1 1) facet of the (3 1 1) step is

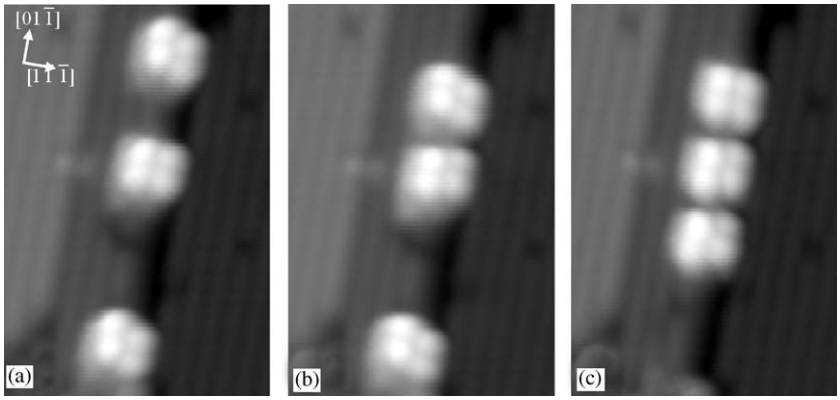

Fig. 42. Lander molecules at a reconstructed step edge (image size: 7 nm × 11 nm). Between (a), (b), and (c) STM lateral manipulations in constant current mode have been performed to form a chain of molecules. The molecules are always oriented with their boards in the [1 −1 0] direction. The distance of neighboring molecules in (c) is 20 Å. Reprinted from Ref. [100]. Copyright 2003, with permission from Elsevier.

extended to a width of three unit cells ($3 \times 4.23\,\text{Å} = 12.7\,\text{Å}$), matching the width of a Lander molecule (15 Å). This explains the selective adsorption at (3 1 1) steps: The mass transport to form a (3 1 1) facet of the size of a Lander molecule is minimal at this step, compared to the (2 1 1) surface or a (1 1 1) step. The molecule is located on the (3 1 1) facet and oriented parallel to the closed packed rows.

The controlled manipulation of Lander molecules along the reconstructed step edges is also possible, as shown in Fig. 42. The molecules do not change their orientation, remaining with the board at the step edge and oriented parallel to the step. The step edge acts as a rail on which the Landers are kept oriented and positioned along a straight line. In Fig. 42, lateral manipulation along a restructured step edge has been used to align three Lander molecules. The distance between the molecules is 20 Å, matching the van der Waals bonding distance. This is the closest distance that could be achieved by lateral manipulation. If a molecule is pushed closer to the next they move both simultaneously, keeping a distance of at least 20 Å. We can conclude that in this conformation the step edge can be utilized as atomically precise guidance to form molecular chains, suggesting how self ordering processes can be combined with Low Temperature STM manipulation to form atomically defined nano-structures from large organic molecules.

10. Electronic contact of a molecular wire with an atomically controlled nanoelectrode

In a molecular device made of a single molecule connected to metallic electrodes, the electronic contacts are unambiguously defined when the edges of the electrodes are atomically ordered, clean and when the geometry of the molecular unit at the junction is under control at the atomic scale. Any deviation from this order increases the electrical resistance of the device. Abandoning atomically clean contact conditions (and not observing the contact region to determine the well connected molecules) leads to characteristics randomly changing from device to device [35], with the consequence that a large increase of the number of molecules per device is necessary to stabilize its electronic functions [121]. In this context, LT-STM is a fundamental technique to study different molecular conformations and to manipulate single molecules, bringing them in electronic interaction with atomically ordered nanoelectrodes. For example, the possibility of bridging a spatial gap between two chains of gold atoms with a copper

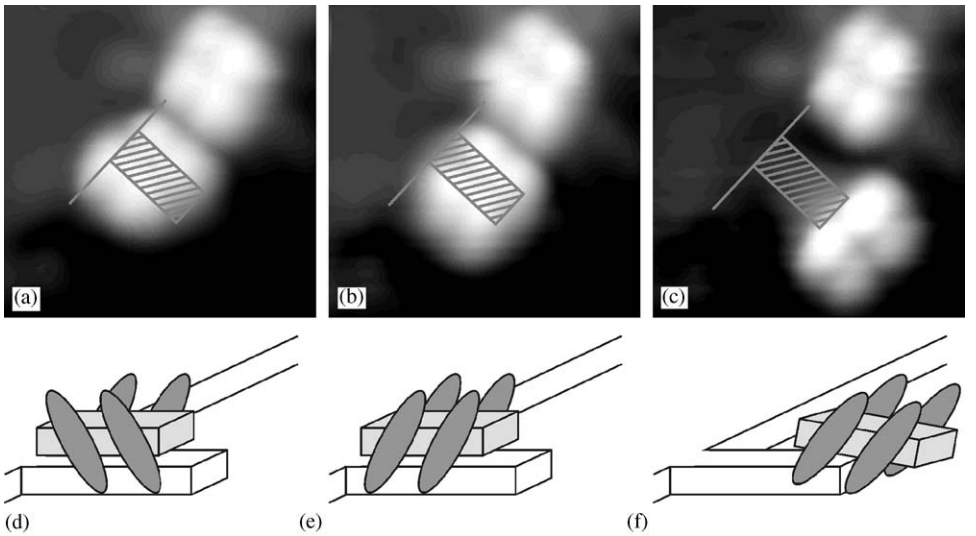

Fig. 43. STM images ($4.5 \times 4.5\,nm^2$) of the initial (a), intermediate (b) and final (c) position of the Lander molecule on the nanostructure. (d)–(f) Corresponding schematic models of a Lander molecule during lateral manipulation along a Cu(1 1 0) tooth. The step edge and the position of the Cu nanostructure underneath the Lander are marked, as determined from an STM image after the removal of the molecule.

phthalocyanine molecule and the formed contact between the molecule and the metal atoms has been shown recently [132].

When adsorbed on a copper terrace, the central wire of the Lander molecule does not contribute to the STM image. It is far away from the surface and its electronic coupling with the metal surface is too weak to be detected. However, we have seen in the previous section that on Cu(1 1 0) the molecule restructures the substrate forming a two atoms wide nanowire under the molecular wire board. In this case the central board is in a good position to interact with the metallic copper wire underneath.

When the molecule is adsorbed at the nanostructure like in Fig. 37, a contrast of about 2 Å is observed for the legs, while the central wire is expected to interact with the copper wire underneath. However, the large contribution of the legs to the tunneling current overshadows the central board contrast. To better observe this small contribution at a given end of the molecular wire, one should choose a conformation of the molecule where the legs contribute as less as possible to the STM tunneling current. This means that the legs have to be oriented to the opposite end of the central wire in order to enable the tip access to this molecular wire end [131].

To obtain this configuration and move a Lander at the end of its Cu atomic wire, the whole molecule is manipulated along the copper nanostructure with the STM tip. In this case, the height of the tip above the surface is decreased during the manipulation, working at a tunneling resistance of about 50 kΩ. The molecule maintains its original board orientation during the whole manipulation process until the end of the wire.

STM images of the Lander molecule have been taken at each manipulation step. Three different positions, shown in Fig. 43(a)–(c), are observed before the molecule is completely pushed away from the tooth. The first position in Fig. 43(a) is the initial one, before manipulation. The Lander is here in

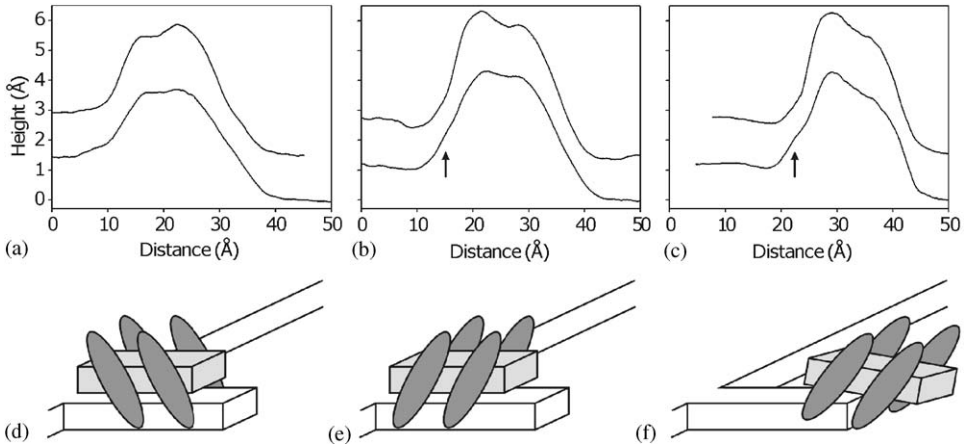

Fig. 44. Experimental linescans across the center (lower curves) and across a pair of legs (shifted upwards by 1.5 Å for clarity) of the Lander molecule in the initial (a), intermediate (b) and final position (c). The arrows indicate shoulders attributed to the central wire. Corresponding models of the molecular conformations are shown in (d–f).

an crossed legs conformation. Only about 10% of the Landers adsorb directly in this conformation. In Fig. 43(c) the molecule has reached the end of the wire: The two lobes close to the Cu wire appear much brighter in the STM image than the other ones, showing that the molecule is tilted with respect to the flat conformations on the nanostructure or on the terrace. Any further tip-induced shift results in a complete removal from the nanostructure leaving the molecule on the lower terrace.

Linescans across the central wire and across the legs are shown in Fig. 44, for the different positions of the Lander along the nanostructure. As one can see, a shoulder in the STM contrast corresponding to the contact position of the molecular board appears when the molecule has been manipulated to the end of the wire (Fig. 44(c)). In this case the legs have a favorable conformation, so that the tip has access to the end naphthalene group of the central wire. The contact shoulder is clearly visible and has an apparent relative height of about 20 pm. Moreover, weaker shoulders are visible in the STM images for intermediate positions [131]. ESQC calculations confirm that an electronic interaction between the board and the metallic Cu atomic wire underneath takes place making the central molecular wire of the Lander visible in the STM images.

Another experiment to investigate the contact between a molecular wire and its electrode, has been performed by the lateral manipulation of a Lander molecule on Cu(1 1 1) [133]. The contact edge of an atomically ordered electrode has been mimicked by a stable and extremely clean mono-atomic step (0.21 nm in height) obtained by a controlled crash of the tip into the surface. As one can see in Fig. 45, the intrinsic steps are irregular and decorated by adsorbates and defects, while the freshly produced steps are free from defects and allow the clear observation of the parallel standing waves pattern produced by the scattering of surface state electrons.

To bring the molecular wire in contact with a fabricated monoatomic step, a Lander molecule lying on the lower terrace (Fig. 46(a)) was laterally manipulated by the STM tip in constant height mode. Knowing the board orientation from the interplay between calculated and the experimental images, one can choose to push the molecule toward the step edge with the central board either parallel or perpendicular to the step.

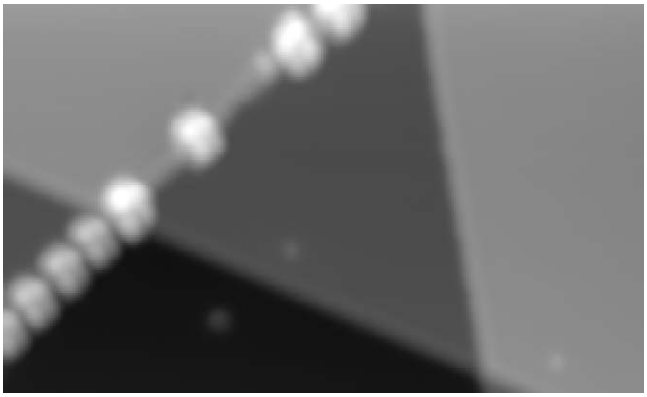

Fig. 45. Clean monoatomic steps formed by a controlled crash of the tip on the surface. The intrinsic step is covered by defects and Lander molecules deposited at room temperature.

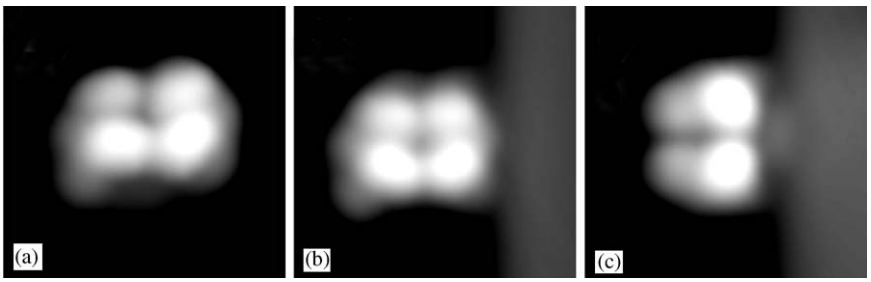

Fig. 46. STM images of a Lander molecule on Cu(1 1 1). (a) Lander on a terrace with the legs in parallel conformation. (b) Lander in contact with a step with the board parallel to it. (c) Lander contacted to a step with the board perpendicular to it. An additional bump corresponding to the contact point of the wire to the step is visible. Image size $3.4 \times 3.4\,\mathrm{nm}^2$. Reprinted with permission from Ref. [133]. Copyright 2003 by the American Physical Society.

When the Lander molecule has its board parallel to the step, two legs are brought into contact with the step edge (Fig. 46(b)). The lower CH_3 groups of two lateral legs are at a van der Waals distance to the step as extracted from STM-ESQC images and molecular mechanics calculations. Separated by the legs, the molecular orbitals of the delocalized electron system of the central wire are not interacting with the step edge.

When the Lander is manipulated to situate its board perpendicularly to the step edge, a bump is visible at the contact position. The STM-ESQC extraction of the corresponding molecular conformation from the experimental image shows that the terminal naphthalene group of the wire is now on top of the step edge and is electronically coupled to the upper terrace. As a consequence, this naphthalene end group is now visible in the STM image of the step edge (Fig. 46(c)).

The conformation of the molecule in different positions with respect to the step edge calculated by MM-ESQC and the corresponding calculated images are reported in Fig. 47. The molecule is in a parallel-leg conformation on the terrace (Fig. 47(a)) and has an average wire height of about 0.36 nm above the surface. Fig. 47(b) and (c) shows the conformation of the molecule when contacted to the step

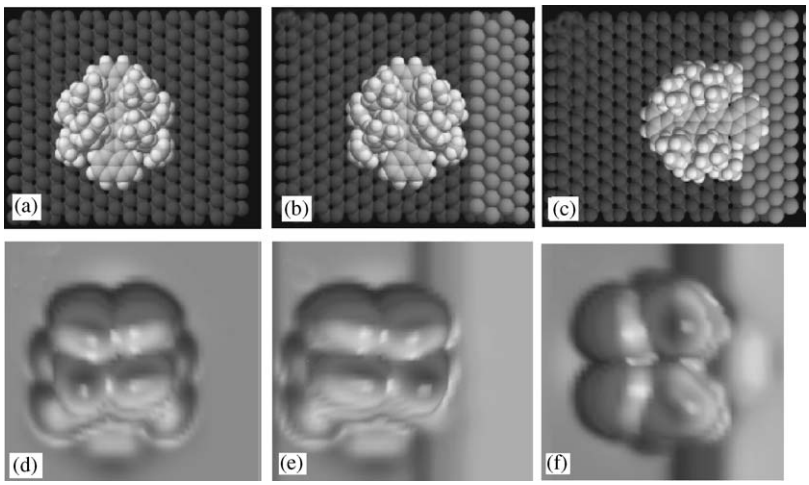

Fig. 47. (a–c) Sphere models of optimized molecular structures. (d–f) Calculated STM images, corresponding to the models above relative to a Lander molecules on a free Cu(1 1 1) surface (a and d) and contacted to a (1 0 0) step of an edge dislocation. The molecule can be contacted with the molecular board parallel ((b) and (e)) or orthogonal ((c) and (f)) to the step. In (f) the additional bump corresponding to the contact point of the wire to the step is visible. Reprinted with permission from Ref. [133]. Copyright 2003 by the American Physical Society.

through the lateral legs or through the board, respectively. Fig. 47(d)–(f) give the corresponding calculated STM images.

The height of the contact bump in the STM images is related to the electronic interaction between the naphthalene end group and the Cu atoms of the upper terrace, but depends first of all on the geometry of the system. It varies as a function of both lateral distance Δx between the naphthalene end group and the step edge and vertical distance z between this end and the upper terrace. At the experimental contact position, it is deduced by calculations that the legs constrain the naphthalene end to stay $z = 0.35$ nm above the upper terrace. For this geometry, a calculated value of the contact bump of 13 pm (in agreement with an experimental value of about 15 pm) is obtained. This value is very small compared, for example, to the corrugation of 100 pm observed by STM for conjugated molecules chemisorbed on the (1 1 1) face of noble metals and can be explained by the relative large z distance of the naphthalene end group from the upper terrace, imposed by the legs.

The discussed contact conformation, reached by STM manipulation at a mono-atomic step edge on Cu(1 1 1), is very similar to the one obtained for the Lander molecule manipulated at the end of the restructured copper wire [131]. In the present case, only the naphthalene end of the molecular wire is positioned to interact with the upper terrace of the Cu(1 1 1) step edge. In the case of Cu(1 1 0), on the other hand, a larger part of the central molecular wire interacts with the Cu atomic wire. The corresponding shoulder characterizes the electronic interaction of the naphthalene end group with the Cu atomic wire with an apparent relative height of about 20 pm, indicating a similar electronic interaction with the atomic wire underneath as in the Cu(1 1 1) case. This interaction may be improved by changing the chemical composition of the wire end while maintaining this peculiar co-facial interaction between the molecular π orbital of the central board and the metallic atomic wire.

11. Probing the contact of a molecular wire by surface electron waves

Electrons occupying surface states on the close-packed surface of noble metals form a two-dimensional nearly free electron gas. The scattering of these electrons off step edges and point defects produces standing wave patterns in the electron density, which can be directly observed by STM at low temperature [134,135].

The principle is quite simple and is theoretically explained in Ref. [136]: electrons tunneling from the tip to a Cu(1 1 1) surface produce a region of enhanced electron amplitude, which travels away from the tip along the surface. If the electron wave encounters a scattering center, such as a step edge or an adatom, it may be scattered and return to the region of the tip, where it will interfere constructively or destructively with the amplitude leaving the tip. The flux of electrons leaving the tip is proportional to the square of the wave function amplitude. The interference therefore will cause oscillations of the current as a function of either energy (determined by the bias voltage) or distance from the defect, both of which affect the phase of the returning wave. From this kind of analysis of the standing wave patterns it is possible to directly determine the surface state dispersion and the scattering properties of the scatterers.

By using atomic manipulation to build artificial structures, it is possible to assemble specific enclosed structure of adatoms (the so called quantum corrals) confining electrons to quantitatively study the scattering properties of the different artificial systems [137,138]. Recently, it was shown that the electronic structure of a single Mn atom placed within a circular corral can be modified by varying the shape of the corral [139]. Moreover, an elliptic quantum corral has been used as an electron mirror to detect, at one ellipse's focus, the spectroscopic Kondo signature of a magnetic atom put in the other focus [140].

Another important point of view on the scattering of the surface state electrons has been focused in our group in Berlin [141], showing that the scattering of the two-dimensional electron gas off step edges and defects, not only has an effect on the standing wave patterns, but also produces itself an interaction between the scatterers. A quantitative study of the long-range interaction between two single copper adatoms on Cu(1 1 1) mediated by the surface state electrons has been performed. The interaction potential was determined by evaluating the distance distribution between two adatoms from a series of STM images taken at temperatures between 9 and 21 K. We found that the long-range interaction is oscillatory with the period of half the Fermi wavelength and decays for larger distances d as $1/d^2$. An example of Cu adatoms deposited on Cu(1 1 1) is shown in Fig. 48. As one can see, the adatoms form islands with a local hexagonal structure and an average distance of 12.5 Å, indicating the existence of an attractive potential minimum between the adatoms at such distance, as well as a potential barrier for dimer formation. An interesting application of this effect has been recently demonstrated by Silly et al. [142]. By means of Cerium atoms on Ag(1 1 1) it has been possible to use such long-range interaction to produce a large ordered atomic superlattice.

Finally, the observation of the standing wave patterns finds another fundamental application in the study of the electronic interaction of the different internal groups of a molecule with the metallic substrate [143] and in particular of the terminal part of a molecular wire with the edge of a Cu(1 1 1) step [133]. The 2D-electron gas, with its wavelength of the order of 1.5 nm, is very sensitive to atomic scale perturbations and it is able to check, in an atomically precise way, the electronic contacting and de-contacting of the wire to a step edge, opening a new way to characterize the electronic contact between a single molecule and its electrodes.

In Fig. 49(a) a Lander molecule on a Cu(1 1 1) terrace in the parallel legs configuration is shown. The Lander adsorption on a clean Cu(1 1 1) terrace perturbs the corresponding 2D electron gas and creates a nearly circular standing wave pattern with a periodicity of about 1.5 nm (measured at $V_{\text{bias}} = 100$ mV)

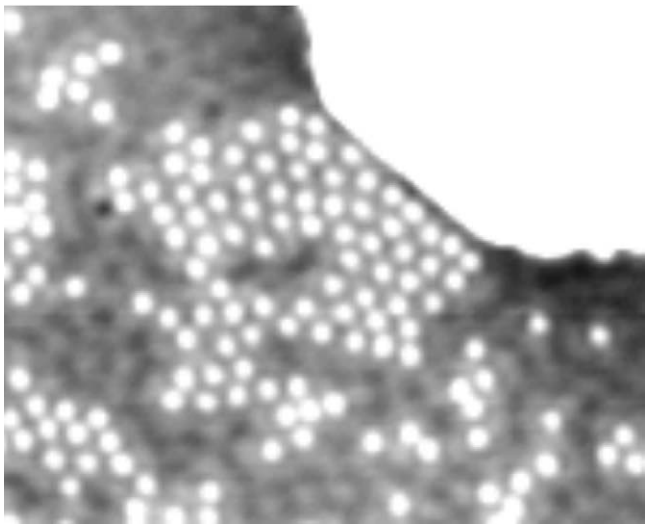

Fig. 48. Single Cu adatoms evaporated at 15 K on Cu(1 1 1). The Cu adatoms form islands with local hexagonal order at an average distance of 12.5 Å. Image size: 200 × 250 Å. Bias voltage: 100 mV. Current: 1.9 nA. Reprinted with permission from Ref. [141]. Copyright 2000 by the American Physical Society.

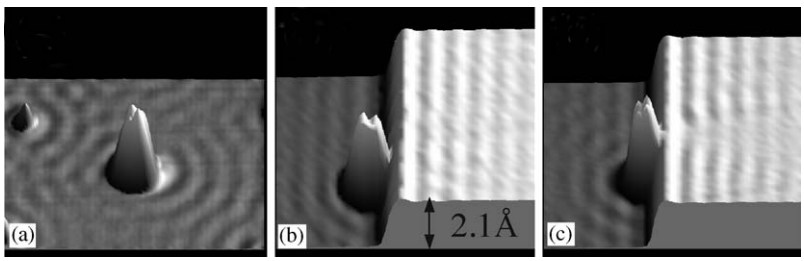

Fig. 49. (a) 3D image of the circular standing wave patterns formed by the molecule on the terrace. (b) Standing wave patterns of a Lander in contact with a step with the board parallel to it. (c) Standing wave patterns corresponding to a Lander contacted to a step with the board perpendicular to it. The parallel pattern in the upper terrace is modified by the contact. Image size $15 \times 12.5\,\mathrm{nm}^2$, standing wave patterns corrugation 0.05 Å. Reprinted with permission from Ref. [133]. Copyright 2003 by the American Physical Society.

around each Lander. No apparent difference in the circular LDOS patterns surrounding the Lander was observed between the parallel and the anti-parallel conformation of the legs.

When the Lander is contacted with its board perpendicularly to the step edge, a striking modification of the standing-wave patterns is observed on the upper terrace (Fig. 49(c)). Compared to the clean step edge case, the amplitude of the standing wave is reduced at the naphthalene contact location. This effect extends a few 10 nm away from the contact in a characteristic triangular shape.

To reproduce the new pattern by calculations, we used the scattering formalism of Heller et al. [136]. In the simulation it is assumed that the scatterers act as ideal black dots, i.e. they have an absorption

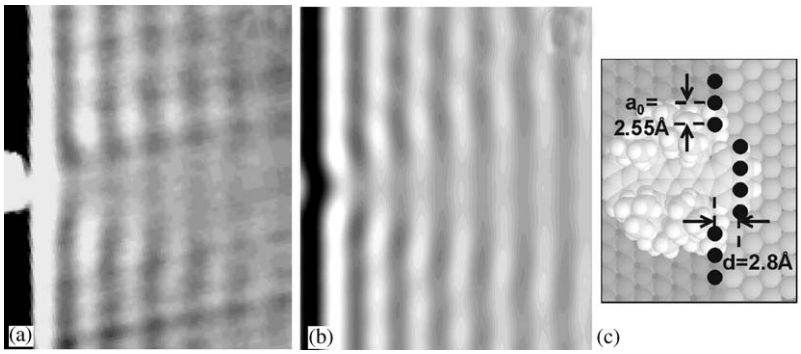

Fig. 50. Electron density patterns in the vicinity of a contacted Lander molecule. (a) Measured image, size $9 \times 11\,\mathrm{nm}^2$. (b) Calculated electron density pattern for a scattering geometry as sketched in (c) using a single scattering approach. (c) Model of the geometry of scatterers used for the calculation (black dots), the model of the molecular mechanics calculation is shown faintly as background for comparison of the two models. Reprinted with permission from Ref. [133]. Copyright 2003 by the American Physical Society.

coefficient of 1. It has been found that the black dot limit [136] is a good approximation for simulating the positions of maxima and minima in standing wave patterns. A simple arrangement of scatterers was used to model the contact: A line of black dots, equally spaced with the nearest-neighbor distance of 2.55 Å, representing the step edge and a number of black dots (N), displaced by a distance (d) perpendicular off the line, representing the contact (Fig. 50(c)). N and d were varied systematically and optimized to obtain best agreement with the experimental data (Fig. 50(a)), leading to $d = 2.8$ Å and $N = 4$. In this case, the calculated pattern (Fig. 50(b)) coincides with the experiment in showing a perturbed region of similar shape descending from the contact point and in this region a decreased wave amplitude and a phase-shift. In this geometry, size and position of the object formed by the black dots reveal the size and position of the molecular board as in Fig. 50(c), as determined by molecular mechanics calculations. This indicates that the perturbation of the standing wave patterns on the upper terrace is caused by the naphthalene end group of the molecular wire. The good agreement between STM experiment and numerical simulation confirms that the molecular π-orbitals of the wire interact with the upper terrace surface state through their coupling via the naphthalene end. This naphthalene acts like an effective 0.76 nm large scattering centre positioned 0.28 nm off the step edge. This 0.28 nm shift is in agreement with the position of the naphthalene end on the upper terrace as deduced from molecular modeling.

The reported experiment shows that the contact between a molecular wire and a step edge can be investigated and controlled at the atomic scale and that the interaction between the terminal part of the wire with the surface electronic states due to the contact notably modifies the electronic standing wave patterns on the upper terrace. The reported characterization of a molecular contact can be now applied to new molecules, where the molecular wire–pad distance is further reduced.

12. Conclusions and outlook

Some of the possibilities offered by the application of LT-STM manipulation to specially designed molecules have been reviewed in this article. We have shown that the manipulation of a single molecule

and the modification of its internal configurations can be achieved by applying the improved manipulation and imaging techniques recently developed in our group.

The selective manipulation of internal parts of a TBPP molecule has been performed demonstrating the principle of a conformational molecular switch. Moreover, the internal mechanics of a molecule during lateral manipulation has been successfully investigated and the small intramolecular changes taking place inside the molecule have been recorded in real time.

Lander molecules deposited onto Cu(1 1 0) and Cu(2 1 1) at room temperature adsorb selectively at step edges and induce a restructuring of the surface underneath the molecular wire board of the Lander. The so-formed nanostructures can be used as atomically precise guidance to form molecular chains. In the case of Cu(1 1 0), such restructuring produces two-atoms-wide nanowires, which can used to investigate the contact of the a Lander molecule. In the STM image, the quality of the contact between the molecular wire and the metallic nanostructure is quantitatively determined by measuring the apparent corrugation at the contact position.

The manipulation of a Lander molecule to a step edge of Cu(1 1 1) offers further possibilities to investigate and control the contact between a molecule and a metallic electrode at the atomic scale. The contact is quantitatively characterized by the apparent height of the contact position in the STM images. Moreover, we have observed that the interaction of the terminal part of the wire with the surface states due to the contact notably modifies the electronic standing wave pattern on the upper terrace.

The reported experiments open the possibility to extend the research in different directions. Our molecular contact characterization technique is for example now in demand of new molecules, able to further reduce the molecular wire-pad distance, and atomically ordered metallic contact pads fabricated on the surface of insulators.

More generally, an important objective is presently to further develop the experimental ability of manipulating single molecules with the aim of using them as nano-machines. So far, efforts have concentrated on understanding the basic mechanisms for moving at will single molecules on a surface. Now a new concept should be elaborated, where molecules are considered not only as elementary building blocks of matter but also as nano-objects or nano-machines in themselves. Using a single molecule as a functionalized nano-machine will require being able to control not only its position but also numerous geometric, electronic, chemical and mechanical parameters at the atomic level, and to be able to progressively increase the complexity of its motion. In this respect, we believe that a significant advance can be achieved due to recent progress in chemical synthesis of large molecules, methods of manipulation with the STM and theoretical modeling.

Another interesting prospective is to further develop the possibility of chemical synthesis at the molecular level, performed by LT-STM manipulation. Chemical reactions on metallic or insulating substrates can be followed step by step and the synthesis of single molecules investigated in detail. The method can then be applied to new molecular structures. Starting from elementary building blocks it will become possible to build complex and precisely designed molecular electronic and mechanical devices.

Acknowledgements

The work presented here has been possible thanks to the fruitful collaboration with Gerhard Meyer, Jascha Repp, Leo Gross, Leonhard Grill, Micol Alemani, André Gourdon, Christian Joachim and Karl Heinz Rieder. Thanks to Christian Roth for technical assistance. Founding by the European Union program

“Atomic and Molecular Manipulation”, the RTN program “AMMIST” and by the Volkswagen Foundation project “Single molecule synthesis” is gratefully acknowledged.

References

[1] G. Binnig, H. Rohrer, Helv. Phys. Acta 55 (1982) 726.
[2] G. Binnig, H. Rohrer, Ch. Gerber, E. Weibel, Phys. Rev. Lett. 49 (1982) 57.
[3] G. Binnig, H. Rohrer, Ch. Gerber, E. Weibel, Phys. Rev. Lett. 50 (1983) 120.
[4] G. Binnig, H. Rohrer, Rev. Mod. Phys. 59 (1987) 615.
[5] J.A. Stroscio, D.M. Eigler, Science 254 (1991) 1319.
[6] Ph. Avouris, Acc. Chem. Res. 28 (1995) 95.
[7] B. Neu, G. Meyer, K.H. Rieder, Mod. Phys. Lett. B 9 (1995) 963.
[8] G. Meyer, J. Repp, S. Zöphel, K.-F. Braun, S.W. Hla, S. Fölsch, L. Bartels, F. Moresco, K.H. Rieder, Single Mol. 1 (2000) 79.
[9] J.K. Gimzewski, C. Joachim, Science 283 (1999) 1683.
[10] T.A. Jung, R.R. Schlitter, J.K. Gimzewski, H. Tang, C. Joachim, Science 271 (1996) 181.
[11] C. Joachim, J.K. Gimzewski, R.R. Schlitter, C. Chavy, Phys. Rev. Lett. 74 (1995) 2102.
[12] J.K. Gimzewski, C. Joachim, R.R. Schlitter, V. Langlais, H. Tang, I. Johannsen, Science 281 (1998) 531.
[13] M.R. Brycs, M.C. Petty, D. Bloor (Eds.), Molecular Electronics, Oxford University Press, New York, 1995.
[14] C. Joachim, J.K. Gimzewski, A. Aviram, Nature 408 (2000) 541.
[15] C. Joachim, Nanotechnology 13 (2002) R1.
[16] A. Aviram, M.A. Ratner, Chem. Phys. Lett. 29 (1974) 277.
[17] S.N. Cohen, Sci. Am. 6 (1975) 24.
[18] D. Freedman, Science 254 (1991) 1308.
[19] S.B. Smith, L. Finzi, C. Bustamante, Science 258 (1992) 1122.
[20] C. Bustamante, Z. Bryant, S.B. Smith, Nature 421 (2003) 423–427.
[21] C. Mao, W. Sun, Z. Shen, N.C. Seeman, Nature 397 (1999) 144.
[22] M.D. Dellow, P.H. Beton, C.J.G.M. Langerak, T.J. Foster, P.C. Main, L. Eaves, M. Henini, S.P. Beaumont, C.D.W. Wilkinson, Phys. Rev. Lett. 68 (1992) 1754.
[23] R.C. Ashoori, H.L. Stormer, J.S. Weiner, L.N. Pfeiffer, S.J. Pearton, K.W. Baldwin, K.W. West, Phys. Rev. Lett. 68 (1992) 3088.
[24] C.P. Collier, R.J. Saykally, J.J. Shiang, S.E. Henrichs, J.R. Heat, Science 277 (1997) 1978.
[25] G. Binnig, C.F. Quate, Ch. Gerber, Phys. Rev. Lett. 56 (1986) 930.
[26] J.K. Gimzewski, E.P. Stoll, R.R. Schlitter, Surf. Sci. 181 (1987) 267.
[27] X.D. Cui et al., Science 294 (2001) 571.
[28] D.M. Eigler, C.P. Lutz, W.E. Rudge, Nature 352 (1991) 600.
[29] C. Joachim, J.K. Gimzewski, Chem. Phys. Lett. 265 (1997) 353.
[30] M. Dorogi, J. Gomez, R. Osifchin, R.P. Andres, R. Reifenberger, Phys. Rev. B 52 (1995) 9071.
[31] J. Park et al., Nature 417 (2002) 722.
[32] W. Liang, M.P. Shores, M. Bockreth, J.R. Long, H. Park, Nature 417 (2002) 725.
[33] M.A. Reed et al., Ann. NY Acad. Sci. 852 (1998) 133.
[34] M.A. Reed, C. Zhou, C.J. Muller, T.P. Burgin, J.M. Tour, Science 278 (1997) 252.
[35] R.H.M. Smit, Y. Noat, C. Untiedt, N.D. Lang, M.C. van Hermert, J.M. van Ruitenbeek, Nature 419 (2002) 906.
[36] C. Kerguelis et al., Phys. Rev. B 59 (1999) 12505.
[37] A. Bezryadin, C. Dekker, G. Schmidt, Appl. Phys. Lett. 71 (1997) 1273.
[38] V. Rousset, C. Joachim, B. Rousset, N. Fabre, J. Phys. III 5 (1995) 1983.
[39] E. Di Fabrizio et al., Jpn. J. Appl. Phys. 36 (1997) L70.
[40] S.J. Tans, A.R.M. Verschueren, C. Dekker, Nature 393 (1998) 59.
[41] S.J. Tans, M.H. Devoret, R.J.A. Groeneveld, C. Dekker, Nature 394 (1998) 761.
[42] T.W. Ebbesen et al., Nature 382 (1996) 54.
[43] R. Martel, T. Schmidt, H.R. Shea, T. Hertel, Ph. Avouris, Appl. Phys. Lett. 73 (1998) 2447.

[44] P.G. Collins, M.S. Arnold, Ph. Avouris, Science 292 (2001) 706.
[45] A. Bachtold et al., Appl. Phys. Lett. 73 (1998) 274.
[46] A.I. Yanson, I.K. Yanson, J.M. Ruitenbeek, Nature 400 (1999) 144.
[47] J. Reichert, R. Ochs, D. Beckmann, H.B. Weber, M. Mayor, H.v. Löhneysen, Phys. Rev. Lett. 88 (2002) 176804.
[48] L. Bartels, G. Meyer, K.H. Rieder, Phys. Rev. Lett. 79 (1997) 697.
[49] M. Böhringer, K. Morgenstern, W.D. Schneider, R. Berndt, F. Mauri, A. De Vita, R. Car, Phys. Rev. Lett. 83 (1999) 324.
[50] G.P. Lopinski, D.D.M. Wayner, R.A. Wolkow, Nature 406 (2000) 48.
[51] Y. Okawa, M. Aono, Nature 409 (2001) 683.
[52] T. Yokoyama, S. Yokoyama, T. Kamikado, Y. Okuno, S. Mashiko, Nature 413 (2001) 619.
[53] G.M. Whitesides, Scient. Am. 9 (1995) 114.
[54] Y. Xia, J.A. Rogers, K.E. Paul, G.M. Whitesides, Chem. Rev. 99 (1999) 1823.
[55] H.G. Craighead, Science 290 (2000) 1532.
[56] S.R. Forrest, Chem. Rev. 97 (1997) 1793.
[57] A.N. Shipway, E. Katz, I. Willner, Chem. Phys. Chem. 1 (2000) 18.
[58] M. Ortega Lorenzo, C.J. Baddeley, C. Muryn, R. Raval, Nature 404 (2002) 376.
[59] B. Kasemo, J. Gold, Adv. Dent. Res. 13 (1999) 8.
[60] J.V. Barth, J. Weckesser, C. Cai, P. Gunter, L. Burgi, O. Jeandupeux, K. Kern, Angw. Chem. Int. Ed. 39 (2000) 1230.
[61] J.M. Tour, M. Kozaki, J.M. Seminario, J. Am. Chem. Soc. 120 (1998) 8486.
[62] J. Chen, M.A. Reed, A.M. Rawlett, J.M. Tour, Science 286 (1999) 1550.
[63] V.J. Langlais, R.R. Schlitter, H. Tang, A. Gourdon, C. Joachim, J.K. Gimzewski, Phys. Rev. Lett. 83 (1999) 2809.
[64] N.D. Lang, Ph. Avouris, Phys. Rev. Lett. 84 (2000) 358.
[65] A. Nitzan, M.A. Ratner, Science 300 (2003) 1384.
[66] G. Meyer, Rev. Sci. Instr. 67 (1996) 2960.
[67] S. Zöphel, Ph.D. Thesis, Freie Universität Berlin, 2000
[68] R. Wiesendanger, Scanning Probe Microscopy and Spectroscopy, University Press, Cambridge, 1994.
[69] J. Tersoff, D.R. Hamann, Phys. Rev. B 31 (1985) 805.
[70] G. Meyer, B. Neu, K.H. Rieder, Appl. Phys. A 60 (1995) 343.
[71] T.W. Fishlock, A. Oral, R.G. Egdell, J.B. Pethica, Nature 404 (2000) 743.
[72] B.G. Briner, M. Doering, H.-P. Rust, A.M. Bradshaw, Science (1997) 257.
[73] L. Bartels, G. Meyer, K.H. Rieder, Appl. Phys. Lett. 71 (1997) 213.
[74] L. Bartels, G. Meyer, K.H. Rieder, Chem. Phys. Lett. 285 (1998) 284.
[75] G. Dujardin, A. Mayne, O. Robert, F. Rose, C. Joachim, H. Tang, Phys. Rev. Lett. 80 (1998) 3085.
[76] G. Dujardin, A. Mayne, F. Rose, Phys. Rev. Lett. 82 (1999) 3448.
[77] L. Bartels, G. Meyer, K.H. Rieder, D. Velic, E. Knoesel, A. Hotzel, M. Wolf, F. Ertl, Phys. Rev. Lett. 80 (1998) 2004.
[78] F. Moresco, G. Meyer, K.H. Rieder, Mod. Phys. Lett. B 13 (1999) 709.
[79] R.M. Feenstra, Surf. Sci. 299 (1994) 965.
[80] B.C. Stipe, A. Rezaei, W. Ho, W. Science 280 (1998) 1732.
[81] W. Ho, J. Chem. Phys. 117 (2002) 11033.
[82] T.M. Wallis, X. Chen, W. Ho, J. Chem. Phys. 113 (2000) 4837.
[83] K. Morgenstern, K.H. Rieder, J. Chem. Phys. 116 (2002) 5746.
[84] L.J. Lauhon, W. Ho, Phys. Rev. Lett. 85 (2000) 4566.
[85] Y. Kim, T. Komeda, M. Kawai, Phys. Rev. Lett. 89 (2002) 126104.
[86] B.G. Briner, et al., unpublished
[87] S.W. Hla, L. Bartels, G. Meyer, K.H. Rieder, Phys. Rev. Lett. 85 (2000) 2777.
[88] N. Nilius, T.M. Wallis, W. Ho, Science 297 (2002) 1853.
[89] A.J. Heinrich, C.P. Lutz, J.A. Gupta, D.M. Eigler, Science 298 (2002) 1381.
[90] S. Chiang, Chem. Rev. 97 (1987) 1083.
[91] P.S. Weiss, D.M. Eigler, Phys. Rev. Lett. 71 (1993) 3139.
[92] J.M. Tour, Chem. Rev. 96 (1996) 537.
[93] K.M. Smith (Ed.), Porphyrins and Metalloporphyrins, Elsevier, New York, 1975.
[94] F. Moresco, G. Meyer, K.H. Rieder, J. Ping, H. Tang, C. Joachim, Surf. Sci. 499 (2002) 94.
[95] T.A. Jung, R.R. Schlitter, J.K. Gimzewski, Nature 386 (1997) 696.

[96] A. Gourdon, Eur. J. Org. Chem. (1998) 2797.
[97] J. Kuntze, R. Berndt, J. Ping, H. Tang, A. Gourdon, C. Joachim, Phys. Rev. B 65 (2002) 233405.
[98] F. Rosei, M. Schunack, P. Jang, A. Gourdon, E. Laegsgaard, I. Stensgaard, C. Joachim, F. Besenbacher, Science 296 (2002) 328.
[99] M. Schunack, F. Rosei, Y. Naitoh, P. Jang, A. Gourdon, E. Laegsgaard, I. Stensgaard, C. Joachim, F. Besenbacher, J. Chem. Phys. 117 (2002) 6259.
[100] L. Gross, F. Moresco, M. Alemani, K.H. Rieder, H. Tang, C. Joachim, Chem. Phys. Lett. 371 (2003) 750.
[101] T. Zambelli, H. Tang, J. Lagoute, S. Gauthier, A. Gourdon, C. Joachim, Chem. Phys. Lett. 348 (2001) 1.
[102] L. Savio, F. Moresco, A. Gourdon, C. Joachim, K.H. Rieder, unpublished
[103] R. Otero, Y. Naitoh, F. Rosei, P. Jiang, P. Thorstrup, A. Gourdon, E. Laegsgaard, I. Stensgaard, C. Joachim, F. Besenbacher, Angew. Chem. Int. Ed. 43 (2004) 2092.
[104] T. Zambelli, P. Jiang, L. Lagoute, S.E. Grillo, S. Gauthier, A. Gourdon, C. Joachim, Phys. Rev. B 66 (2002) 075410.
[105] F. Moresco, G. Meyer, K.H. Rieder, H. Tang, A. Gourdon, C. Joachim, Appl. Phys. Lett. 78 (2001) 306.
[106] F. Moresco, G. Meyer, H. Tang, C. Joachim, K.H. Rieder, J. Electron Spectrosc. Relat. Phenom. 129 (2003) 149.
[107] P. Sautet, C. Joachim, Chem. Phys. Lett. 185 (1991) 23.
[108] P.H. Lippel, R.J. Wilson, M.D. Miller, Ch. Wöll, S. Chiang, Phys. Rev. Lett. 62 (1989) 171.
[109] D.P.E. Smith, J.K.H. Hörber, G. Binnig, H. Nejoh, Nature 344 (1990) 641.
[110] J. Tersoff, D.R. Hamann, Phys. Rev. Lett. 50 (1983) 1998.
[111] J. Bardeen, Phys. Rev. Lett. 6 (1961) 57.
[112] N.D. Lang, Phys. Rev. Lett. 56 (1986) 1164.
[113] N.D. Lang, Phys. Rev. B 34 (1986) 5947.
[114] P. Sautet, C. Joachim, Surf. Sci. 271 (1992) 387.
[115] X. Boujiu, C. Joachim, C. Girard, Phys. Rev. B 59 (1999) R7845.
[116] C. Joachim, H. Tang, F. Moresco, G. Rapenne, G. Meyer, Nanotechnology 13 (2002) 330.
[117] G. Jimenez-Bueno, G. Rapenne, Tetrahedron Lett. 44 (2003) 6261.
[118] B.L. Feringa (Ed.), Molecular Switches, Wiley-VCH, Weinheim, 2001.
[119] Z.J. Donhauser, B.A. Mantooth, K.F. Kelly, L.A. Bumm, J.D. Monnell, J.J. Stapleton, D.W. Price Jr., A.M. Rawlett, D.L. Allara, J.M. Tour, P.S. Weiss, Science 292 (2001) 2303.
[120] M. di Ventra, S.T. Pantelides, N.D. Lang, Appl. Phys. Lett. 76 (2000) 3448.
[121] C.P. Collier, E.W. Wong, M. Belohradský, F.M. Raymo, J.F. Stoddart, P.J. Kuekes, R.S. Williams, J.R. Heath, Science 285 (1999) 391.
[122] C.P. Collier, G. Mattersteig, E.W. Wong, Y. Luo, K. Beverly, J. Sampaio, F.M. Raymo, J.F. Stoddart, J.R. Heath, Science 289 (2000) 1172.
[123] G.K. Ramachandran, T.H. Hopson, A.M. Rawlett, L.A. Nagahara, A. Primak, S.M. Lindsay, Science 300 (2003) 1413.
[124] F. Moresco, G. Meyer, K.H. Rieder, H. Tang, A. Gourdon, C. Joachim, Phys. Rev. Lett. 86 (2001) 672.
[125] A.R.H. Clarke, J.B. Pethica, J.A. Nieminen, F. Besenbacher, E. Laegsgaard, I. Stensgaard, Phys. Rev. Lett. 76 (1996) 1276.
[126] L. Olesen, M. Brandbyge, M.R. Soresen, K.W. Jacobsen, E. Laegsgaard, I. Stensgaard, F. Besenbacher, Phys. Rev. Lett 76 (1996) 1485.
[127] Ch. Loppacher, M. Guggisberg, O. Pfeiffer, E. Meyer, M. Bammerlin, R. Lüthi, R. Schlitter, J.K. Gimzewski, H. Tang, C. Joachim, Phys. Rev. Lett. 90 (2003) 066107.
[128] F. Moresco, G. Meyer, K.H. Rieder, H. Tang, A. Gourdon, C. Joachim, Phys. Rev. Lett. 87 (2001) 088302.
[129] M. Schunack, L. Petersen, A. Kühnle, E. Laegsgaard, I. Stensgard, I. Johannsen, F. Besenbacher, Phys. Rev. Lett. 86 (2001) 456.
[130] J. Weckesser, C. Cepek, R. Fasel, J.V. Barth, F. Baumberger, T. Greber, K. Kern, J. Chem. Phys. 115 (2001) 9001.
[131] L. Grill, F. Moresco, P. Jiang, C. Joachim, A. Gourdon, K.H. Rieder, Phys. Rev. B 69 (2004) 035416.
[132] G.V. Nazin, X.H. Qiu, W. Ho, Science 302 (2003) 77.
[133] F. Moresco, L. Gross, M. Alemani, K.H. Rieder, H. Tang, A. Gourdon, C. Joachim, Phys. Rev. Lett. 91 (2003) 36601.
[134] M.F. Crommie, C.P. Lutz, D.M. Eigler, Nature 363 (1993) 524.
[135] Y. Hasegawaand, Ph. Avouris, Phys. Rev. Lett. 71 (1993) 1071.
[136] E.J. Heller, M.F. Crommie, C.P. Lutz, D.M. Eigler, Nature 369 (1994) 464.
[137] M.F. Crommie, C.P. Lutz, D.M. Eigler, Nature 262 (1993) 218.

[138] K.-F. Braun, K.H. Rieder, Phys. Rev. Lett. 88 (2002) 096801.
[139] J. Kliewer, R. Berndt, S. Crampin, Phys. Rev. Lett. 85 (2000) 4936.
[140] H.C. Manoharan, C.P. Lutz, D.M. Eigler, Nature 403 (2000) 512.
[141] J. Repp, F. Moresco, G. Meyer, K.H. Rieder, P. Hyldgaard, M. Persson, Phys. Rev. Lett. 85 (2000) 2981.
[142] F. Silly, M. Pivetta, M. Ternes, F. Patthey, J.P. Pelz, W.-D. Schneider, Phys. Rev. Lett. 92 (2004) 016101.
[143] L. Gross, F. Moresco, L. Savio, A. Gourdon, C. Joachim, K.H. Rieder, Phys. Rev. Lett. 93 (2004) 56103.